Geochemistry of adakites and rhyolites from the Neoarchaean Gadwal greenstone belt, eastern Dharwar craton, India: implications for sources and geodynamic setting

C. Manikyamba, R. Kerrich, Tarun C. Khanna, and D.V. Subba Rao

Abstract: Adakite and rhyolite volcanic flows with different petrographic and geochemical characteristics have been identified from the Neoarchaean Gadwal greenstone terrane of the eastern Dharwar craton, India. These are part of the bimodal basalt–felsic association that dominates the belt, which includes previously documented boninites and Nb-enriched basalts. Adakites plot in the MgO–SiO_2 field of Cenozoic adakites, distinct from high-Mg andesites, and have low Yb (1.2 ppm) and fractionated rare-earth elements (REE) (La/Yb_n = 16) of Cenozoic counterparts. They also possess the Cr/Ni (1.3–4.0), Nb/Ta (8.6–12.8), and Zr/Sm (33–58) ratios distinctive of adakites from recent oceanic arcs. Zero to positive Eu anomalies contrast with negative Eu present in older Dharwar cratonic crust, such that crustal contamination is unlikely, endorsing an intraoceanic setting. Cenozoic oceanic adakites may form by slab melting, then hybridizing to variable degree with wedge peridotite, and Gadwal adakites are also interpreted to be slab melts. Rhyolites have greater SiO_2, highly incompatible elements (Th, La, Zr), and higher Yb (2.41 ppm) contents than adakites, with fractionated REE and pronounced negative Eu anomalies; they are comparable to FI type rhyolites of other Archean greenstone belts, likely melts of thick mafic crust at ~40 km with residual garnet, in an extensional setting. Consequently, the switch from arc basalts and boninites to adakites, Nb-enriched basalt, and rhyolites in the Gadwal terrane signifies a transition from slab dehydration-wedge melting to slab melting-wedge hybridization, possibly triggered by ridge subduction or flattening of the slab, as well as crustal melting. These new observations endorse the emergence of complex arc magmatism in Neoarchean terranes.

Résumé : Des écoulements volcaniques d'adakite et de rhyolite ayant différentes caractéristiques pétrographiques et géochimiques ont été identifiés dans le terrane de roches vertes Gadwal (Néoarchéen) de l'est du craton de Dharwar, en Inde. Ils forment une partie de l'association bi-modale felsique-basalte qui domine la ceinture, laquelle comprend des boninites, documentées antérieurement, et des basaltes enrichis en Nb. Les adakites se retrouvent dans le champ MgO–SiO_2 des adakites du Cénozoïque, distinctes des andésites riches en Mg; leur teneur en Yb (1,2 ppm) et en terres rares fractionnées (La/Yb_n =16) est faible par rapport à leurs contreparties du Cénozoïque. Elles ont aussi des rapports distinctifs d'adakites provenant d'arcs océaniques récents, soit Cr/Ni (1,3–4,0), Nb/Ta (8,6–12,8) et Zr/Sm (33–58). Des anomalies Eu zéro à positives contrastent avec les valeurs Eu négatives retrouvées dans la croûte cratonique Dharwar plus ancienne; il en découle donc qu'une contamination crustale est peu probable, appuyant l'hypothèse d'un environnement intra-océanique. Les adakites océaniques datant du Cénozoïque ont pu se former par fusion de dalles, puis s'hybrider à divers degrés avec des coins de péridotites; les adakites de Gadwal sont aussi interprétées comme des fusions de dalles. Les rhyolites ont des teneurs en SiO_2, en éléments hautement incompatibles (Th, La, Zr) et en Yb (2,41 ppm) plus élevées que les adakites, avec des terres rares fractionnées et des anomalies Eu négatives prononcées; elles sont comparables aux rhyolites FI d'autres ceintures de roches vertes archéennes, probablement des fusions de croûte mafique épaisse à ~ 40 km avec du grenat résiduel dans un environnement de distension. Par conséquent, le passage de basaltes d'arc et de boninites à des adakites-basaltes enrichis en Nb, puis à des rhyolites dans le terrane de Gadwal signifie une transition de déshydratation de dalles – fusion de prismes à une fusion de dalles - hybridation de prismes, possiblement déclenchée par une subduction de crêtes ou un aplanissement de la dalle ainsi qu'une fusion de la croûte. Ces nouvelles observations appuient l'émergence de magmatisme d'arc complexe dans les terranes néoarchéens.

[Traduit par la Rédaction]

Received 13 March 2007. Accepted 12 June 2007. Published on the NRC Research Press Web site at cjes.nrc.ca on 13 November 2007.

Paper handled by Associate Editor J. Greenough.

C. Manikyamba,[1] T.C. Khanna, and D.V. Subba Rao. National Geophysical Research Institute, Uppal Road, Hyderabad, 500 007, India.
R. Kerrich. Department of Geological Sciences, University of Saskatchewan, Saskatoon, SK S7N 5E2, Canada.

[1]Corresponding author (e-mail: cmaningri@yahoo.com).

Introduction

Adakites are igneous rocks of intermediate composition originally identified from Adak island, in the Aleutians intraoceanic arc (Defant and Drummond 1990). Relative to "normal" andesites–dacites of oceanic arcs, adakites are distinctive in terms of high MgO at a specified SiO_2; high contents of Cr, Co, Ni, in conjunction with low Y and Yb contents; and pronounced fractionation of heavy rare-earth elements (HREE) (Drummond et al. 1996; Defant and Kepezhinskas 2001; Martin et al. 2005).

According to some authors, adakites are melts of basaltic ocean crust of lithospheric slabs subducting in convergent margins (Martin 1986; Martin et al. 2005, and references therein). Experimental melts of hydrous basalts, over a range of pressure–temperature (*P–T*) conditions, yield compositions less magnesian at a given SiO_2 content than adakites. Accordingly, given their convergent margin setting, adakites are thought to involve a second stage whereby basalt slab melts hybridize with the peridotitic sub-arc mantle wedge during ascent to the crust (Martin 1986; Martin et al. 2005).

In Cenozoic oceanic arcs where adakites have been identified, they are typically associated closely in space and time with the tholeiitic to calc-alkaline basalt–andesite–dacite–rhyolite (BADR) association. Given that the former are likely slab melts, but the latter slab-dehydration wedge melts and their fractionation products, there is a significant transition in thermal regime and geodynamic setting between these two magma series (Drummond et al. 1996; Pearce and Peate 1995). Conventionally, adakites are discriminated from "normal" intermediate compositions on diagrams of La/Yb versus Yb or Sr/Y versus Y (Martin 1986; Drummond et al. 1996; Condie 2005).

In some Cenozoic arcs, there is also an association of adakites with one or more of high-Mg andesites (HMA) and Nb-enriched basalts (NEB). If adakites are slab melts hybridized with mantle-wedge peridotites, then Mg-andesites are likely melts of hybridized peridotite, and NEB are likely melts of the peridotitic residue of Mg-andesites (Sajona et al. 1996; Kepezhinskas et al. 1996). Adakites and Mg-andesites, characterized by a pronounced compositional gap, have been termed high-silica adakites (HSA) and low-silica adakites (LSA), respectively, by Martin et al. (2005); the former are compositionally similar to Archean high-Al tonalites, although adakites are volumetrically small and syn-arc, whereas tonalites are batholithic and syn- to post-tectonic in greenstone belts (Polat and Kerrich 2006).

Igneous rocks with adakite-like compositions have also been reported from Phanerozoic continental arcs, where there is significant assimilation – fractional crystallization (AFC; DePaolo 1980) with continental crust. During AFC, involving crustal assimilation and fractional crystallization of hornblende + titanite, mafic parental melts may evolve into intermediate compositions and trend into the adakite field on diagrams of La/Yb versus Yb or Sr/Y versus Y (Kay et al. 1991; Haschke et al. 2002; Richards and Kerrich in press).

Adakites are part of the dominantly bimodal arc basalt and dacite–rhyolite association of the Neoarchean Gadwal greenstone belt, eastern Dharwar craton. High precision analyses are reported for 14 rhyolites and 10 adakites. These, and existing data for the belt, are used to evaluate an intraoceanic or continental margin setting for the eruption of the lavas and a primary adakite origin versus AFC composition. Petrogenetic processes for adakites and rhyolites are compared. Given a probable intraoceanic setting and primary origin, we then compare Gadwal adakites to other documented occurrences in Neoarchean greenstone terranes.

Given their convergent margin plate tectonic setting in Cenozoic arcs, and increasingly reported occurrence in Archean greenstone belts, the documentation of Archean adakites is important for addessing the question of whether a modified form of Phanerozoic plate tectonics operated in the Archean (see Polat and Kerrich 2006 for a review). Adakites, like boninites, were originally thought to be restricted to Phanerozoic convergent margins. Recognition of both volcanic types in Archean terranes sheds new light on Archean magmatic processes (Kerrich et al. 1998; Hollings and Kerrich 2000; Manikyamba et al. 2005; Manikyamba and Khanna 2005; Naqvi et al. 2006; Polat and Kerrich 2006).

Geological setting

The Dharwar craton of Peninsular India is composed of greenstone belts ranging in age from 3.4 to 2.7 Ga. This craton is divided into eastern and western sectors by the central corridor of ~2.5 Ga Closepet granites (Naqvi and Rogers 1987; Fig. 1A). The eastern sector has smaller dimension greenstone belts with prevalent calc-alkaline bimodal volcanic rocks and subordinate metasedimentary rocks, whereas large greenstone belts consisting of predominantly metasedimentary rocks and the komatiite–tholeiitic basalt association, with minor bimodal volcanic associations, dominate the western sector. Contacts between different greenstone belts and adjacent granites are inferred to be either tectonic or intrusive (Naqvi and Rogers 1987; Ramakrishnan 2003).

Recent geochemical studies of diverse volcanic and sedimentary sequences endorse differences of lithological associations and compositions, and therefore likely distinct geodynamic settings between greenstone belts of the eastern Dharwar craton (EDC) and the western Dharwar craton (WDC). In the EDC belts, volcanic flows have compositions characteristic of hydrous magmas of convergent margin settings: (*i*) the conjunction of a depleted mantle component, light rare-earth element (LREE) enrichment, with high field-strength element (HFSE: Th, Nb, Ta, Ti) anomalies, represented by arc tholeiitic to calc-alkaline basalts and boninites; and (*ii*) NEBs and adakites characteristic of slab melting in convergent margins of Cenozoic intraoceanic arcs (e.g., Sajona et al. 1996). In contrast, komatiite–tholeiitic basalt associations of WDC belts are compositionally depleted mantle erupted from anhydrous mantle plumes in a within-plate setting (Jayananda et al. 2000; Manikyamba et al. 2005; Manikyamba and Khanna 2005; Naqvi et al. 2002, 2006); this is in keeping with the plume model for some greenstone belts (Abbott 1996).

The Gadwal greenstone belt (GGB) is one belt, or terrane, of the larger composite Narayanpet–Gadwal major belt, or accretionary superterrane (NGST), of the EDC. The NGST

Fig. 1. (A) Simplified geological map of southern peninsular India showing the location of the Gadwal greenstone belt relative to other greenstone belts of the eastern Dharwar craton and the Clospet granites that divide the eastern and western Dharwar sectors. (B) Generalized geological map of the Gadwal greenstone belt (after Srinivasan 1990), with the sampling localities.

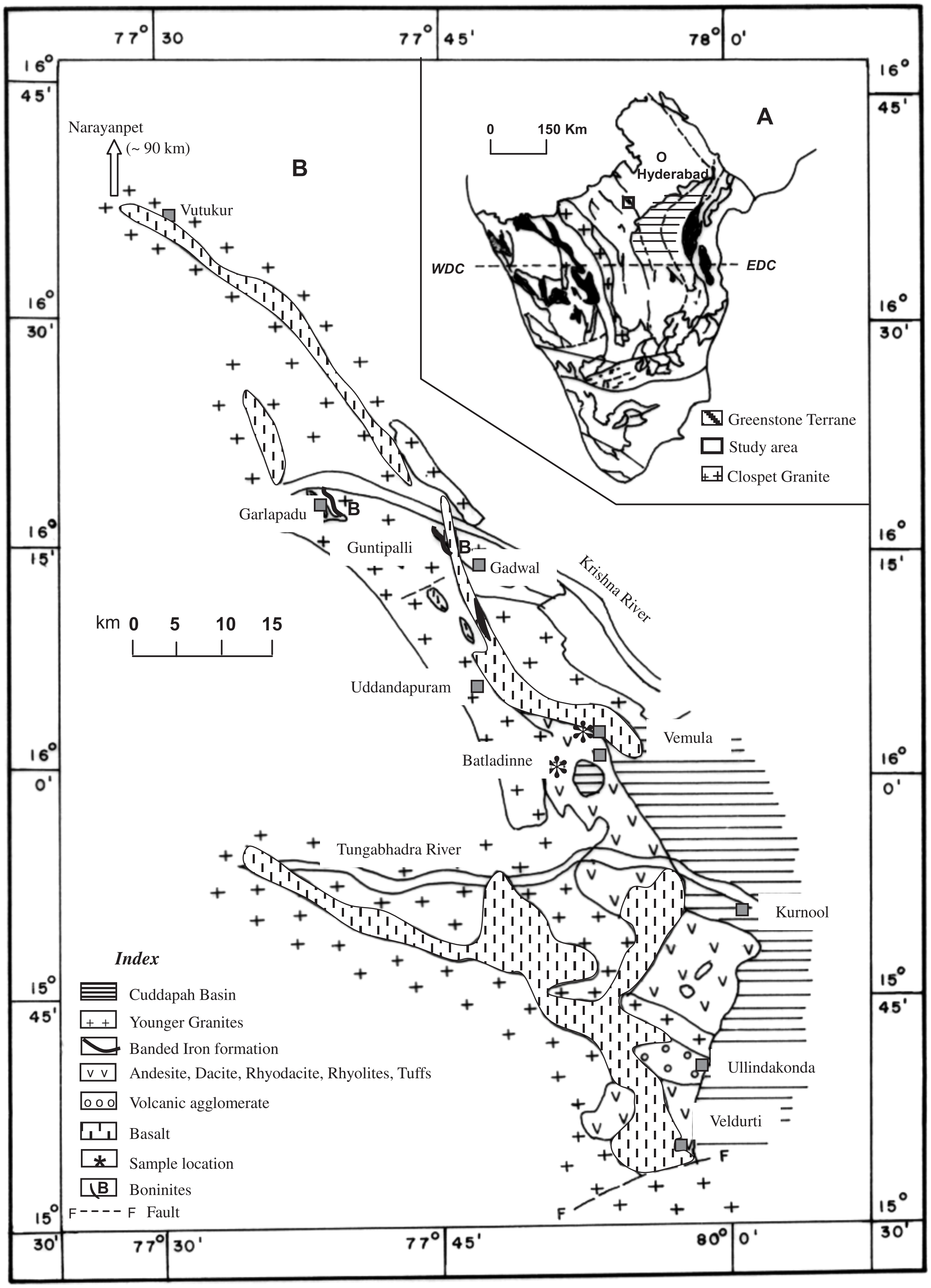

extends north–south from Narayanpet to Veldurti; bimodal volcanic sequences predominate (Fig. 1B). In the north at Guntipalli, an extensive metabasalt sequence includes flows of boninite and NEB composition, and a metre thick adakite flow is interlayered with the boninites (Manikyamba and Khanna 2007). To the south, andesites, HMA, dacites, rhyodacites, and rhyolites are prevalent, with minor arc basalts; these are likely part of an intact stratigraphic succession, but tectonic interleaving of lithologies cannot be ruled out (Figs. 1B, 2; Manikyamba et al. 2005).

The belt has been subjected to three phases of deformation and metamorphosed to amphibolite facies (Matin 2001).

Fig. 2. Generalized tectonostratigraphic section of the Gadwal greenstone terrane, with age constraints (Chalapathi Rao et al. 1999; Jayananda et al. 2000; Anand et al. 2003). Illustrated are the volcanic lithologies, their relative abundance, and interpreted stratigraphic succession at Vemula and Batladinne, where adakites and rhyolites were sampled. Sloping units of adakite and Nb-enriched basalt signify non-layer-cake volcanic stratigraphy.

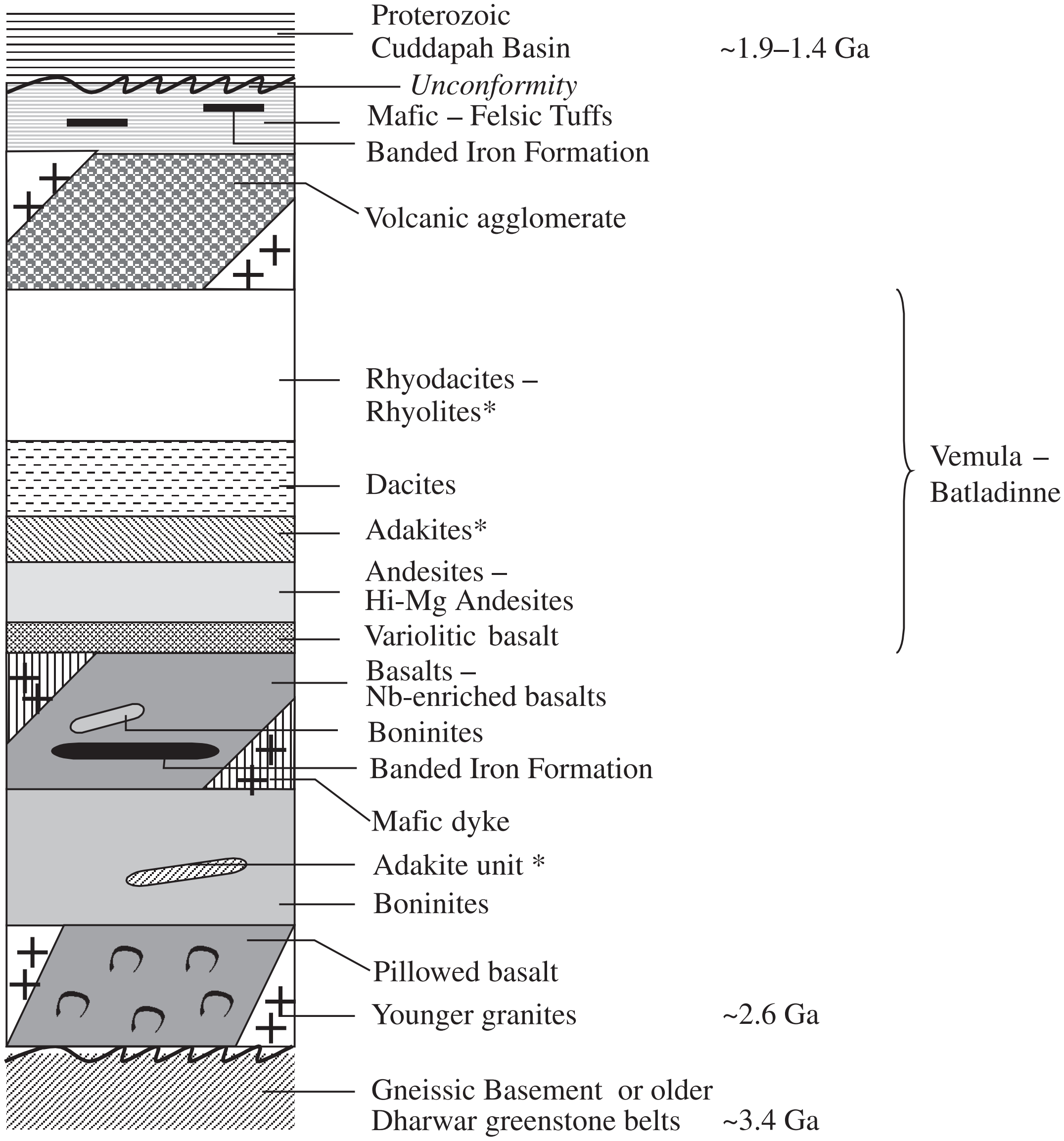

The prefix meta is implicit below for all lithologies. Radiometric ages are not available for volcanic lithologies. Volcanic units of the adjacent Kolar and Ramagiri belts are both ~2.7 Ga, and granites intruding the NGST are ~2.6 Ga, endorsing a Neoarchean age for the Gadwal greenstone terrane (Balakrishnan et al. 1990; Zachariah et al. 1995; Jayananda et al. 2000).

Mineralogically, rhyolites and adakites are distinct in well-preserved phenocrysts of K-feldspar in the former, but of plagioclase in the latter. Rhyolites are predominantly quartz and K-feldspar, plagioclase, with minor biotite partially altered to sericite. Adakites consist of quartz, plagioclase, hornblende, and biotite. Relict plagioclase phenocrysts are present in many sections, but they are partially altered to sericite. Both rock types have apatite, zircon, titanite, and titano-magnetite as accessory minerals.

Sampling and analytical techniques

Samples were obtained from unweathered outcrop near Vemula and Batladinne (Fig. 1B). The tectonostratigraphic section in Fig. 2 illustrates the relationships of adakites and rhyolites to basalts. This is interpreted as an intact volcanic sequence, but tectonic interleaving cannot be ruled out. After petrographic screening, a subset of least-altered samples was selected for geochemical studies. Rocks were powdered using an agate mortar. Major elements were analyzed by X-ray flourescence (XRF; Phillips MAGIX PRO Model 2440), with relative standard deviations <3%. For rare-earth elements (REE), HFSE, and other trace elements, powders were dissolved in reagent grade HF and HNO_3 in Savillex screw-top vessels, using the procedure of Longerich et al. (1990) and Jenner et al. (1990), and determined by inductively coupled plasma – mass spectyrometry (ICP–MS; Perkin Elmer SCIEX ELAN DRC II) at the National Geophysical Research Institute, Hyderabad, India. BHVO-1, JB-2, and JR-1 were run as reference materials; precision and accuracy are better than 5% for the majority of trace elements (Balaram and Gnaneswar Rao 2003).

Results

Screening for alteration

Elemental mobility may be a problem in the study of metamorphosed and deformed volcanic rocks; therefore, it is essential to address the effects of alteration on the geochemistry of Archean volcanic rocks for understanding their petrogenesis (Polat et al. 2002, and references therein). Least-altered samples were identified in the field by preservation of volcanic structures, low state of deformation, and absence of carbonate or sulphide overprint, and petrographically on the basis of preserved igneous textures and minimal pseudomorphing of primary igneous phases.

Alteration insensitive elements, including Al, Ti, Y, other HFSE, REE (except Ce and Eu), Sc, and V, have been used to infer the primary compositional characteristics of Archean volcanic rocks, whereas large-ion lithophile elements (LILE: Cs, Ba, Rb, K), Sr, and Pb are generally mobile (Humphris and Thompson 1978; Kerrich and Fryer 1979; Dostal et al. 1980; Ludden et al. 1982; Murphy and Hynes 1986; Jochum et al. 1991; Lafleche et al. 1992; Arndt 1994). When HFSE and REE (Th, Zr, Yb) are plotted with Sm, adakites and rhyolites form distinct linear interelement trends (not shown). MgO and SiO_2 may be mobile during intense hydrothermal alteration. Such alteration can be ruled out both by the preservation of igneous textures and the separate data clusters for adakites and rhyolites (Fig. 3) that also include the alteration insensitive element Nb. Furthermore, Polat et al. (2002) demonstrated that rocks having Ce/Ce* ratios between 0.9 and 1.1 display limited LREE mobility, whereas those with Ce/Ce* <0.9 or >1.1 are characterized by significant LREE mobility. This ratio clusters at 1.0–1.1 in both adakites and rhyolites of the present study and, taken with coherent REE patterns, endorses limited mobility of REE. We note in addition the coherent, but distinct, primitive mantle normalized diagrams of the two populations, as well as their coherent but different Eu anomalies, signifying low mobility of those elements (see later in the text).

Major and trace element relationships

Based on petrography and geochemistry, these rocks have been divided into adakites and rhyolites. Adakites have systematically lower SiO_2 and greater Al_2O_3, TiO_2, and Fe_2O_3 relative to rhyolites, as well as greater contents of mafic-affiliated (Cr, Co, Ni, Sc, V) elements (Tables 1, 2). Adakites plot mostly within the adakite (HSA) field of Martin et al. (2005) in SiO_2 versus MgO coordinates such that these elements were little affected by alteration (Fig. 3). However, CaO and Na_2O are scattered. All but two samples have much greater K_2O than the adakite average of 1.97 wt.%, and Sr/Y ratios are consistently lower than the adakite average of 56 indicative of Sr loss (Tables 1, 2, 3).

Fig. 3. Plots of (A) MgO versus SiO_2 and (B) Nb versus SiO_2 for adakites and rhyolites of the Gadwal greenstone terrane. The field of high-silica adakites (HSA = adakites) and average low-silica adakites (LSA = high-Mg andesites) are from Martin et al. (2005). avg., average.

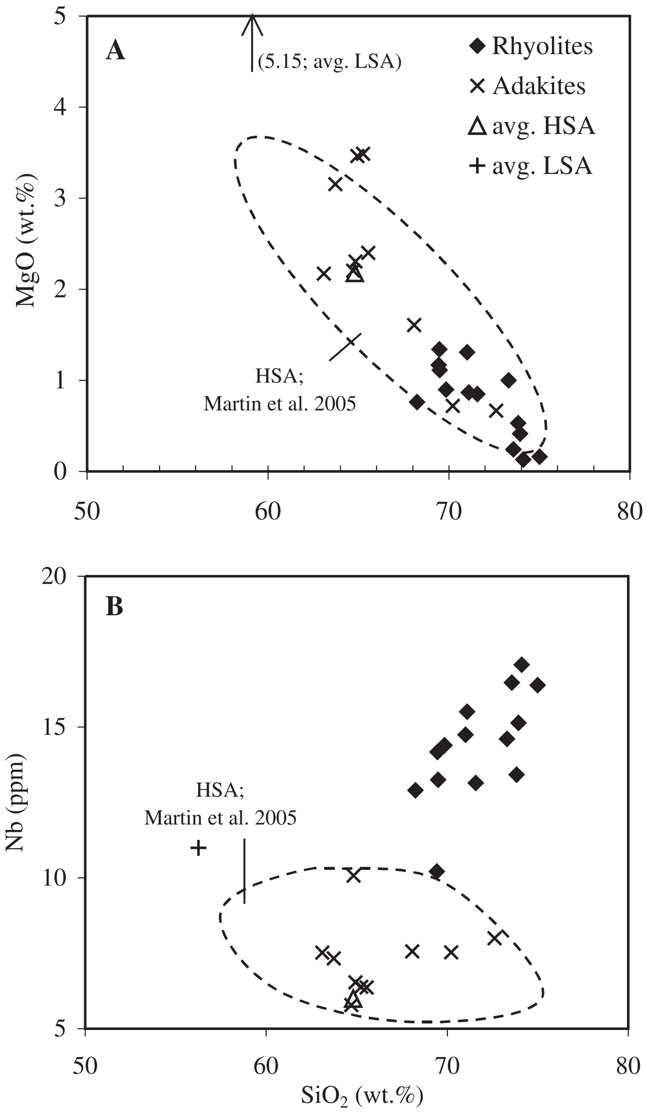

Adakites possess lower LREE, Y, and HREE than rhyolites and smooth patterns from La to Ho. Adakites have zero to positive Eu anomalies consistent with minor plagioclase accumulation, whereas rhyolites are distinctive in pronounced negative Eu anomalies (Fig. 4; Tables 1, 2). On REE and primitive mantle normalized diagrams, relative to rhyolites, adakites are characterized by systematically: (*i*) lower contents of highly incompatible (Th, U, Nb, Ta), (*ii*) moderately incompatible (Zr, Hf, Gd), (*iii*) compatible (Y, Yb) elements, as well as (*iv*) smaller Ti anomalies (Figs. 4, 5; Tables 1, 2).

Defant and Kepezhinskas (2001) set the following criteria for adakites, with the Gadwal average data in brackets: SiO_2 >56 wt.% (66.3), Al_2O_3 >15 wt.% (15.4), Y <18 ppm (15), Yb <1.9 ppm (1.2), and La/Yb_n >20 (16). Accordingly, these samples qualify as adakites on four out of five counts. How-

Table 1. Chemical composition of adakites from the Gadwal greenstone belt.

	G65	G68	G69	G71	G72	G77	G79	G80	G76	G78
SiO_2	72.61	64.93	65.25	65.54	70.22	63.73	64.83	63.09	64.70	68.07
TiO_2	0.22	0.51	0.50	0.52	0.30	0.68	0.64	0.58	0.47	0.56
Al_2O_3	16.18	15.38	15.39	16.24	17.09	12.70	16.47	16.32	13.52	14.32
Fe_2O_3	2.42	6.13	5.59	5.54	2.42	6.93	5.38	6.80	7.31	5.48
MnO	0.05	0.08	0.08	0.07	0.05	0.07	0.06	0.10	0.09	0.05
MgO	0.67	3.46	3.49	2.40	0.72	3.15	2.30	2.17	2.20	1.61
CaO	3.81	4.20	5.04	5.22	2.72	5.48	4.07	6.37	6.57	5.56
K_2O	0.92	0.22	0.27	0.68	0.99	1.33	1.47	0.57	1.91	1.47
Na_2O	3.06	4.93	4.24	3.65	5.39	3.70	4.55	3.83	3.08	2.68
P_2O_5	0.05	0.16	0.15	0.13	0.10	0.22	0.22	0.16	0.14	0.19
Mg#	0.35	0.53	0.55	0.46	0.37	0.47	0.46	0.39	0.37	0.37
Cr	2.21	26.64	27.75	9.25	1.81	27.54	14.50	15.86	4.54	15.45
Co	5.15	15.99	16.37	14.66	3.69	19.75	13.61	16.78	16.18	12.67
Ni	0.94	11.07	11.12	5.09	0.70	6.80	5.96	6.24	3.46	6.01
Rb	84	18	27	34	73	50	90	21	74	70
Sr	146	181	178	267	142	420	402	297	274	203
Cs	18.5	0.8	1.4	5.6	11.9	4.1	38.4	1.2	11.4	4.6
Ba	284	111	84	243	202	475	426	121	437	234
Sc	2.6	10.3	9.9	10.6	3.7	12.1	9.7	9.7	10.9	7.8
V	22	139	138	138	22	191	154	178	190	123
Ta	0.71	0.67	0.65	0.74	0.63	0.58	0.79	0.76	0.54	0.70
Nb	8.0	6.5	6.4	6.4	7.5	7.3	10.1	7.5	5.8	7.6
Zr	150	157	154	162	159	150	185	160	151	163
Hf	3.5	3.5	3.4	3.6	3.7	3.2	3.9	3.5	3.2	3.5
Th	15	8	7	9	11	8	11	7	7	9
U	3.0	1.5	1.4	2.1	2.5	1.5	2.4	1.7	1.8	2.2
Y	10	14	14	17	12	18	18	19	16	16
La	33.54	20.96	20.45	22.09	26.58	30.18	34.54	20.28	21.93	26.39
Ce	56.17	39.72	37.96	39.47	46.18	55.62	63.60	38.47	38.14	48.21
Pr	5.20	4.04	3.88	3.98	4.43	5.90	6.73	4.13	3.89	5.01
Nd	17.76	15.48	14.99	15.05	15.71	23.25	26.96	16.52	15.60	19.53
Sm	2.82	3.12	2.98	3.20	2.74	4.60	5.15	3.63	3.23	3.84
Eu	1.38	0.98	0.81	0.93	0.85	1.38	1.48	1.11	0.97	1.36
Gd	2.28	2.62	2.60	2.78	2.29	3.68	4.00	3.16	2.66	3.07
Tb	0.32	0.43	0.40	0.46	0.35	0.56	0.58	0.54	0.42	0.48
Dy	1.46	2.10	2.06	2.42	1.64	2.64	2.65	2.77	2.16	2.21
Ho	0.24	0.37	0.36	0.43	0.29	0.45	0.45	0.50	0.39	0.40
Er	0.83	1.15	1.15	1.39	0.93	1.43	1.37	1.57	1.31	1.26
Tm	0.13	0.18	0.18	0.22	0.15	0.21	0.21	0.24	0.20	0.19
Yb	0.79	1.15	1.11	1.43	0.98	1.34	1.24	1.54	1.26	1.18
Lu	0.13	0.17	0.17	0.22	0.16	0.21	0.20	0.24	0.20	0.18
Total REE	123	92	89	94	103	131	149	95	92	113
Cu	1.85	5.31	9.81	11.10	1.33	8.05	13.51	3.67	2.21	4.96
Zn	22	51	48	67	30	79	61	65	67	50
Tl	0.36	0.10	0.13	0.15	0.34	0.17	0.42	0.09	0.24	0.26
Pb	17	23	22	24	19	25	26	19	17	19
Sb	0.44	0.37	0.26	0.54	0.39	1.15	1.87	0.67	1.15	2.45
La/Nb	4.20	3.21	3.20	3.47	3.53	4.12	3.43	2.70	3.79	3.49
Nb/Ta	11.3	9.8	9.9	8.6	12.0	12.6	12.8	9.8	10.8	10.8
Zr/Sm	53.3	50.1	51.7	50.6	58.0	32.6	36.0	44.1	47.0	42.4
Th/Ce	0.3	0.2	0.2	0.2	0.2	0.1	0.2	0.2	0.2	0.2
$(La/Yb)_n$	30.3	13.0	13.2	11.1	19.5	16.2	20.0	9.4	12.5	16.0
$(La/Sm)_n$	7.5	4.2	4.3	4.3	6.1	4.1	4.2	3.5	4.3	4.3

Table 1 (*concluded*).

	G65	G68	G69	G71	G72	G77	G79	G80	G76	G78
(Gd/Yb)n	2.4	1.9	1.9	1.6	1.9	2.3	2.7	1.7	1.8	2.2
Eu/Eu*	1.6	1.0	0.9	0.9	1.0	1.0	1.0	1.0	1.0	1.2
Ce/Ce*	1.0	1.1	1.0	1.0	1.0	1.0	1.0	1.0	1.0	1.0
Cr/Ni	2.3	2.4	2.5	1.8	2.6	4.0	2.4	2.5	1.3	2.6
Zr/Hf	42.6	45.0	45.6	45.0	43.4	47.1	47.0	45.7	48.0	46.3
Zr/Y	14.5	11.0	11.0	9.5	13.4	8.4	10.5	8.3	9.6	10.5
Ti/Sm	459	974	997	982	664	891	745	957	880	872

Note: All the values are recalculated to 100% volatile free. REE, rare-earth elements.

ever, Martin et al. (2005) set La/Yb_n >15 for adakites, so there is some latitude in compositional definitions (see Richards and Kerrich (2007) for a compilation of adakite definitions). In contrast, rhyolites have SiO_2 (71.7 wt.%) too high, but Al_2O_3 (14.4 wt.%) too low for compliance with the adakite definition (Tables 1, 2, 3).

According to Martin et al. (2005), Cr/Ni ratios, which are fractionation dependent in HSA, may discriminate between LSA (1–2.5) and HSA (0.5–4.5). Gadwal adakites exhibit similarities with HSA in their Cr/Ni of 1.3–4, in keeping with SiO_2–MgO relationships and depleted Yb of adakites (Fig. 3; Table 1, one outlier).

Discussion

Intraoceanic or continental margin setting

Negative Eu anomalies are characteristic of Mesoarchean crust of the Dharwar craton (Gao and Wedepohl 1995; Naqvi 2005). Zero to positive Eu anomalies of adakites provide the most direct line of evidence that the adakites have not been contaminated by older continental crust known to be present locally in the Dharwar craton and, accordingly, were likely erupted in an intraoceanic setting (Fig. 4). Contamination by contemporaneous crust is possible; however, Nb, Y, and Yb contents are too low and $(Gd/Yb)_n$ and Th/Ce ratios too high for any significant assimilation of Archean upper continental crust (cf. Taylor and McLennan 1985). Independent evidence for an oceanic setting of the Gadwal greenstone terrane is that basalts of the bimodal association plot on the low Ce–Yb array of Recent intraoceanic arcs, such as the South Sandwich Islands (cf. Hawkesworth et al. 1993), and cluster on plots rather than on a mixing array between the most primitive members and continental crust (Manikyamba and Khanna 2007). This is also true of primitive arc basalts in the contemporaneous 2.7 Ga Ramagiri–Hungund greenstone belt (Manikyamba et al. 2004, fig. 8).

Petrogenesis

A worldwide correlation between the age of subducting lithosphere and the composition of arc magmas has been documented. Subduction of younger lithosphere (<30 Ma) produce tonalites, trondhjemites, and dacites having low Yb (<1.9 ppm) and Y (<18 ppm) contents, consistent with their derivation from partial melting of basaltic crust of the slab with residual garnet. Similarly, adakitic magmas are generated because of subduction of young and hot lithospheric slab (Martin 1986; Defant and Drummond 1990; Drummond and Defant 1990; Knowles 1995; Maury et al. 1996; Samaniego 1997). This interpretation is substantiated by adakites of Circum Pacific subduction zones where young oceanic lithosphere has produced active adakitic magmatism (Morris 1995; Maury et al. 1996; Martin 1999; Foley et al. 2000; see Richards and Kerrich 2007 for a review).

Subduction of the older lithosphere (>30 Ma) generates basalts, andesites, dacites, and rhyolites (BADR) by slab dehydration-wedge melting without residual garnet, and these rocks have Yb (>2 ppm) and Y contents varying from 20 to 25 ppm (Pearce and Peate 1995). Gadwal adakites have low Yb (0.79–1.54 ppm) and strongly fractionated HREE, in common with all adakites, indicative of residual garnet (Tables 1, 2). In view of the significance of La and Yb (and Sr/Y in unaltered rocks) in adakites, different workers (Martin 1986, 1999; Drummond and Defant 1990) used a plot of La/Yb versus Yb to separate adakites and tonalites from intermediate to felsic compositions of “normal” tholeiitic to calc-alkaline arc-magma series. Gadwal adakites, and other adakites from the Sandur and Kushtagi greenstone belt, Dharwar craton, all plot in the adakite field at low Yb but with variable $(La/Yb)_n$ (Fig. 6A; Manikyamba and Khanna 2005; Naqvi et al. 2006).

Rapp et al. (1999) conducted experimental studies on natural hydrous basalts at 1–4 GPa and compared the experimental slab melts with adakites from the Philippines, southern Andes, central America, and northern Japan. They concluded that low-Mg# adakites (and HSA) are consistent with slab melting source, whereas high-Mg# adakites (and LSA) are derived from a hybrid and (or) mantle source and establish a clear cut relationship between the slab melt and hybrid melt on the basis of their SiO_2 and Mg# (see Moyen and Stevens 2006 for a recent review). Gadwal adakites are low-Mg# type HSA, plotting with the field of slab melts at 1–4 GPa of Rapp et al. (1999) and the slab-melt field of Smithies et al. (2003).

Low Ni and Cr contents (0.7–11 and 1–28 ppm, respectively) of the Gadwal adakites indicate slab melts reached the surface without significant reaction with mantle peridotite. Gutscher et al. (2000) attribute the low Ni content of some adakites to the absence of mantle-wedge peridotite between the slab and overlying arc crust in a shallow and flat subduction zone.

Table 2. Chemical composition of rhyolites from the Gadwal greenstone belt.

	G84	G87	G88	G91	G95	G96	G99	G100	G102	G103	G104	G105	G74	G85
SiO_2	71.57	73.93	73.56	73.83	75.00	74.11	73.30	69.50	69.47	71.10	71.01	69.84	69.43	68.24
TiO_2	0.46	0.28	0.31	0.27	0.20	0.19	0.43	0.44	0.50	0.45	0.40	0.57	0.38	0.42
Al_2O_3	12.70	14.01	14.26	13.68	13.53	14.06	13.24	14.14	14.62	14.67	13.92	14.96	16.96	16.66
Fe_2O_3	5.44	1.90	1.44	1.86	1.30	0.92	3.02	4.58	3.67	2.74	3.16	3.17	3.54	4.22
MnO	0.08	0.03	0.04	0.06	0.05	0.04	0.05	0.08	0.08	0.05	0.07	0.06	0.06	0.07
MgO	0.85	0.41	0.24	0.53	0.16	0.13	1.00	1.11	1.34	0.87	1.31	0.90	1.17	0.76
CaO	4.03	1.06	0.43	0.98	0.52	0.25	0.74	0.90	2.59	1.81	1.85	1.84	4.38	4.65
K_2O	2.92	4.41	5.35	6.32	5.69	7.60	4.23	7.13	4.20	4.40	4.68	4.93	0.86	1.49
Na_2O	1.85	3.90	4.34	2.41	3.52	2.68	3.86	2.01	3.40	3.77	3.48	3.54	3.15	3.36
P_2O_5	0.11	0.06	0.03	0.06	0.02	0.02	0.13	0.11	0.13	0.13	0.11	0.19	0.08	0.11
Mg#	0.24	0.30	0.25	0.36	0.20	0.22	0.40	0.32	0.42	0.39	0.45	0.36	0.40	0.26
Cr	0.83	10.98	1.74	5.09	1.37	1.52	8.85	4.76	8.88	5.70	4.71	7.88	0.99	11.16
Co	3.79	3.66	0.52	3.95	0.44	0.88	5.17	7.64	7.61	5.31	5.16	6.31	4.50	4.88
Ni	0.54	2.13	0.73	1.57	0.78	0.96	3.60	2.79	2.59	1.81	1.97	1.90	0.76	3.89
Rb	113	144	177	228	182	217	126	248	159	165	144	192	45	87
Sr	125	169	67	141	64	68	101	199	269	235	175	265	112	101
Cs	7.6	3.2	2.3	9.9	2.3	2.9	1.0	6.0	1.7	1.9	1.2	4.6	4.1	7.2
Ba	275	532	803	523	180	198	758	660	810	744	796	824	277	101
Sc	10.1	4.4	4.9	4.7	3.2	3.2	5.7	5.6	6.3	5.4	5.0	6.7	7.4	9.9
V	29	37	9	37	5	6	55	73	79	62	53	89	9	41
Ta	1.19	1.31	1.30	1.35	1.38	1.47	1.27	1.14	1.28	1.25	1.25	1.18	1.09	1.04
Nb	13.2	15.1	16.5	13.4	16.4	17.1	14.6	13.2	14.2	15.5	14.7	14.4	10.2	12.9
Zr	282	235	354	159	254	250	299	273	263	303	290	278	245	274
Hf	6.2	6.0	7.9	4.5	6.6	6.7	6.8	6.2	6.1	7.0	6.6	6.4	5.6	5.9
Th	11	22	25	23	27	27	26	22	26	28	28	25	15	10
U	2.6	5.2	5.7	5.9	5.9	6.3	4.6	5.7	6.9	7.6	5.0	6.5	2.3	2.4
Y	46	29	28	21	28	27	25	26	25	26	24	25	26	43
La	34.71	54.98	88.88	38.88	51.14	49.79	56.13	58.81	56.14	62.35	58.36	59.53	34.81	29.90
Ce	67.20	105.58	158.92	72.59	98.02	96.54	107.50	110.99	105.74	116.48	109.51	112.38	60.87	59.80
Pr	7.39	11.21	16.10	7.32	10.24	10.03	11.09	11.56	10.89	12.18	11.23	11.67	6.16	6.67
Nd	30.27	42.41	58.19	26.66	37.32	35.92	41.05	42.72	40.35	45.47	42.06	44.00	23.36	27.96
Sm	6.92	8.01	9.05	5.06	6.78	6.79	7.15	7.59	7.20	7.83	7.57	7.80	4.67	6.32
Eu	1.67	1.01	1.68	0.79	0.66	0.63	1.49	1.31	1.59	1.58	1.53	1.67	1.17	1.71
Gd	6.13	6.04	6.87	3.86	5.34	5.28	5.46	5.59	5.31	5.79	5.31	5.67	4.05	5.79
Tb	1.11	0.92	0.92	0.61	0.82	0.78	0.79	0.79	0.76	0.81	0.77	0.81	0.66	1.03
Dy	6.22	4.24	4.19	3.05	3.94	3.85	3.76	3.81	3.58	3.80	3.58	3.77	3.54	5.71
Ho	1.15	0.75	0.70	0.53	0.69	0.67	0.63	0.65	0.61	0.67	0.63	0.62	0.65	1.11
Er	3.74	2.32	2.27	1.73	2.29	2.16	2.05	2.13	1.99	2.15	1.99	2.05	2.18	3.63
Tm	0.60	0.37	0.35	0.28	0.37	0.35	0.32	0.33	0.32	0.33	0.31	0.31	0.35	0.58
Yb	3.91	2.27	2.37	1.88	2.38	2.32	2.12	2.18	2.05	2.13	2.05	2.04	2.35	3.73
Lu	0.60	0.36	0.38	0.28	0.38	0.37	0.33	0.34	0.31	0.34	0.31	0.31	0.37	0.56
Total REE	172	240	351	164	220	216	240	249	237	262	245	253	145	155

Table 2 (*concluded*).

	G84	G87	G88	G91	G95	G96	G99	G100	G102	G103	G104	G105	G74	G85
Cu	2.05	4.31	1.23	1.59	1.02	1.29	8.58	12.23	3.65	4.19	2.87	5.00	1.79	2.65
Zn	61	45	49	39	35	29	67	61	55	49	49	54	33	44
Tl	0.32	0.72	0.74	1.11	0.77	1.03	0.54	1.10	0.64	0.64	0.64	0.86	0.19	0.28
Pb	23	23	26	32	25	25	39	40	29	25	22	22	24	21
Sb	0.83	1.38	1.73	1.32	0.88	0.82	0.97	1.04	1.49	5.54	0.96	0.66	0.90	0.72
La/Nb	2.64	3.63	5.39	2.90	3.12	2.92	3.84	4.44	3.96	4.02	3.96	4.14	3.41	2.32
Nb/Ta	11.1	11.5	12.7	9.9	11.9	11.6	11.5	11.6	11.0	12.4	11.8	12.2	9.3	12.4
Zr/Sm	40.7	29.3	39.1	31.4	37.5	36.9	41.8	36.0	36.6	38.7	38.3	35.6	52.4	43.4
Th/Ce	0.2	0.2	0.2	0.3	0.3	0.3	0.2	0.2	0.2	0.2	0.3	0.2	0.2	0.2
(La/Yb)n	6.4	17.4	26.9	14.9	15.4	15.4	18.9	19.4	19.6	20.9	20.4	20.9	10.6	5.8
(La/Sm)n	3.1	4.3	6.1	4.8	4.7	4.6	4.9	4.8	4.9	5.0	4.8	4.8	4.7	3.0
(Gd/Yb)n	1.3	2.2	2.4	1.7	1.9	1.9	2.1	2.1	2.1	2.2	2.1	2.3	1.4	1.3
Eu/Eu*	0.8	0.4	0.6	0.5	0.3	0.3	0.7	0.6	0.8	0.7	0.7	0.7	0.8	0.8
Ce/Ce*	1.0	1.0	1.0	1.1	1.0	1.1	1.1	1.0	1.0	1.0	1.0	1.0	1.0	1.0
Cr/Ni	1.5	5.2	2.4	3.2	1.8	1.6	2.5	1.7	3.4	3.1	2.4	4.2	1.3	2.9
Zr/Hf	45.8	39.4	45.0	35.3	38.8	37.5	44.0	44.3	43.5	43.2	44.2	43.4	43.9	46.2
Zr/Y	6.1	8.2	12.7	7.6	9.2	9.4	11.9	10.7	10.7	11.5	11.9	11.0	9.4	6.3
Ti/Sm	402	212	206	320	178	168	364	351	420	347	319	435	492	399

Note: All the values are recalculated to 100% volatile free. REE, rare-earth elements.

Zr/Sm and Nb/Ta relationships

Drummond et al. (1996) documented Zr/Sm ratios variably greater than primitive mantle values of 25 in high-Al tonalites; this was attributed to melting of an amphibolitic basaltic source. In an extension of this work, Foley et al. (2002) showed that adakites and tonalites are characterized also by Nb/Ta ratios less than the primitive mantle value of 17 and that the Zr/Sm and Nb/Ta systematics can only be accounted for by melting of low-Mg amphibolite of basaltic crust, not high-magnesian amphibolites of cumulates in thick basaltic crust or amphibolite-bearing peridotites. Gadwal adakites plot in the adakite–tonalite field (Fig. 6B; Foley et al. 2002). According to Foley et al. (2002), low values of Nb/Ta result from distribution coefficients between the melt and residual phases, whereas Rapp et al. (2003) infer low values to be a source feature.

However, according to Condie (2005), in contrast to tonalite–trondhjemite–granodiorite (TTG), adakites have Nb/Ta and Zr/Sm that cluster about the respective primitive mantle values of 17 and 25, respectively (Sun and McDonough 1989), reflecting the melting of rutile-bearing eclogite. That adakite field may include suites that are not true adakites (see later in the text).

Adakites: alternative models

Mafic magmas of "normal" tholeiitic to calc-alkaline arc-magma series may acquire adakite-like values of La/Yb, Yb and Sr/Y, Y. Mafic magmas evolve to intermediate compositions by AFC, involving crustal assimilation coupled to fractional crystallization of hornblende and titanite, most typically in continental arcs, lowering Y and Yb contents to adakite-like values. However, such fractionated intermediate compositions, well represented in the Andes, feature listric-shaped REE patterns compared with the smoothly fractionated patterns of adakites (Kay et al. 1991; Richards et al. 2001; Haschke et al. 2002; Klepeis et al. 2003). Given crustal contamination, such fractionated magmas are also characterized by Sr-, Nd-, and Pb-isotope compositions more evolved than depleted upper-mantle values of mid-ocean ridge basalts (MORB) and adakites from oceanic arcs (see Richards and Kerrich (2007) for a review). This is also the case for the Archean sanukitoid series of the western Superior Province, which has compositional similarities to adakites. Stevenson et al. (1999) show that incompatible element enriched Mg-diorites evolve to more felsic products by AFC involving hornblende and titanite, where LREE patterns become steeper but HREE do not, generating listric patterns.

Evidence for an intraoceanic setting of the Gadwal arc-basalt–adakite association has been discussed earlier in the text. The coherence of the Gadwal adakite REE patterns over a range of absolute abundances confers additional evidence that AFC has not been significant. As well, they possess Nb/Ta and Zr/Hf ratios in common with adakites, whereas normal arc magmas are characterized by scattered Nb/Ta and Zr/Sm <25 (Fig. 6B; Foley et al. 2002). Consequently, they are likely primary adakites.

An alternative concept for adakites involves melting of basaltic dykes emplaced into lithospheric mantle peridotite (Macpherson et al. 2006; Melcher and Meisel 2004). If this process operates, it is constrained by empirical observation

Fig. 4. Plots of Th (A), Zr (B), Yb (C), and Ti/Sm (D) versus Eu/Eu*. Symbols as in Fig. 3.

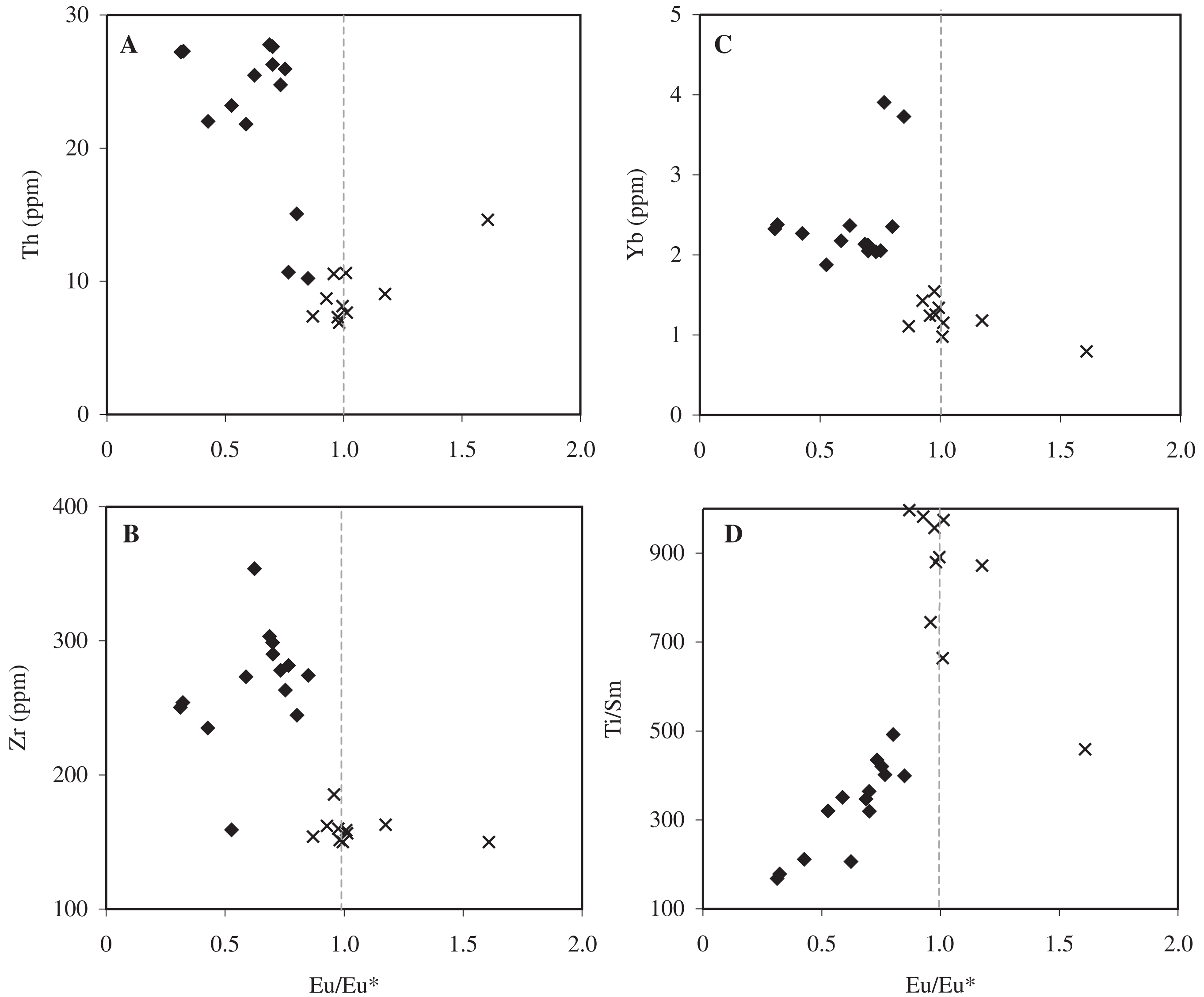

to subduction of crust <30 Ma (Drummond and Defant 1990). Models for high-Al tonalitic batholiths of greenstone belts, with compositions similar to adakites, include melting of thick sequences of crustal basalts (Whalen et al. 2002), melting of thick ocean-plateau crust (Condie 2005), or catalytic delamination of eclogite (Bedard 2006). Adakites of the Gadwal terrane are associated with "classic" intraoceanic-arc lithologies: to the north, boninites and arc basalts; to the south, the association arc BADR. Batholithic tonalites are not spatially and temporally related with those "classic" arc-volcanic associations, and consequently the alternative models are not discussed further here.

Rhyolites

Rhyolites are the Archean FI type of Lesher et al. (1986), characterized by low Yb and fractionated REE. According to Hart et al. (2004), Archean FI rhyolites are interpreted as melts of thick basaltic crust, with garnet–pyroxene–amphibole present, at ~40 km, in a regime of attenuated lithosphere and concurrent high heat flow. Rhyolites cannot be fractionation products of adakites because (*i*) there is no continuum of Eu anomalies between the two populations; (*ii*) rhyolites possess greater highly incompatible-, moderately incompatible-, and compatible-element contents than adakites; (*iii*) rhyolites and adakites have similar LREE fractionations rather than steeper patterns in the former expected from a comagmatic relationship by fractional crystallization; and (*iv*) rhyolites possess lower contents of Cr, Co, Ni (Fig. 5; Tables 1, 2; cf. Richards and Kerrich 2007). Nor are they direct fractionation products of the basaltic end member of the bimodal magma series of the Gadwal greenstone terrane that feature near flat REE patterns (Hart et al. 2004; Manikyamba et al. 2005; Manikyamba and Khanna 2005).

Coeval eruption of two magma series may have involved slab melting for adakites, and melting of the base of arc crust under extension for rhyolites (cf. Hart et al. 2004). Rhyolites of similar adakite-like REE patterns have been reported from the 3 Ga Lumby Lake greenstone belt, Superior Province, which is associated with intermedate to felsic calc-alkaline suites (Hollings and Wyman 1999, type1 felsics).

Fig. 5. Chondrite normalized REE (A, B) and trace element variation (C, D) diagrams for Gadwal rhyolites and adakites. Normalizing values from Sun and McDonough (1989). Samples representing the range of REE contents are plotted.

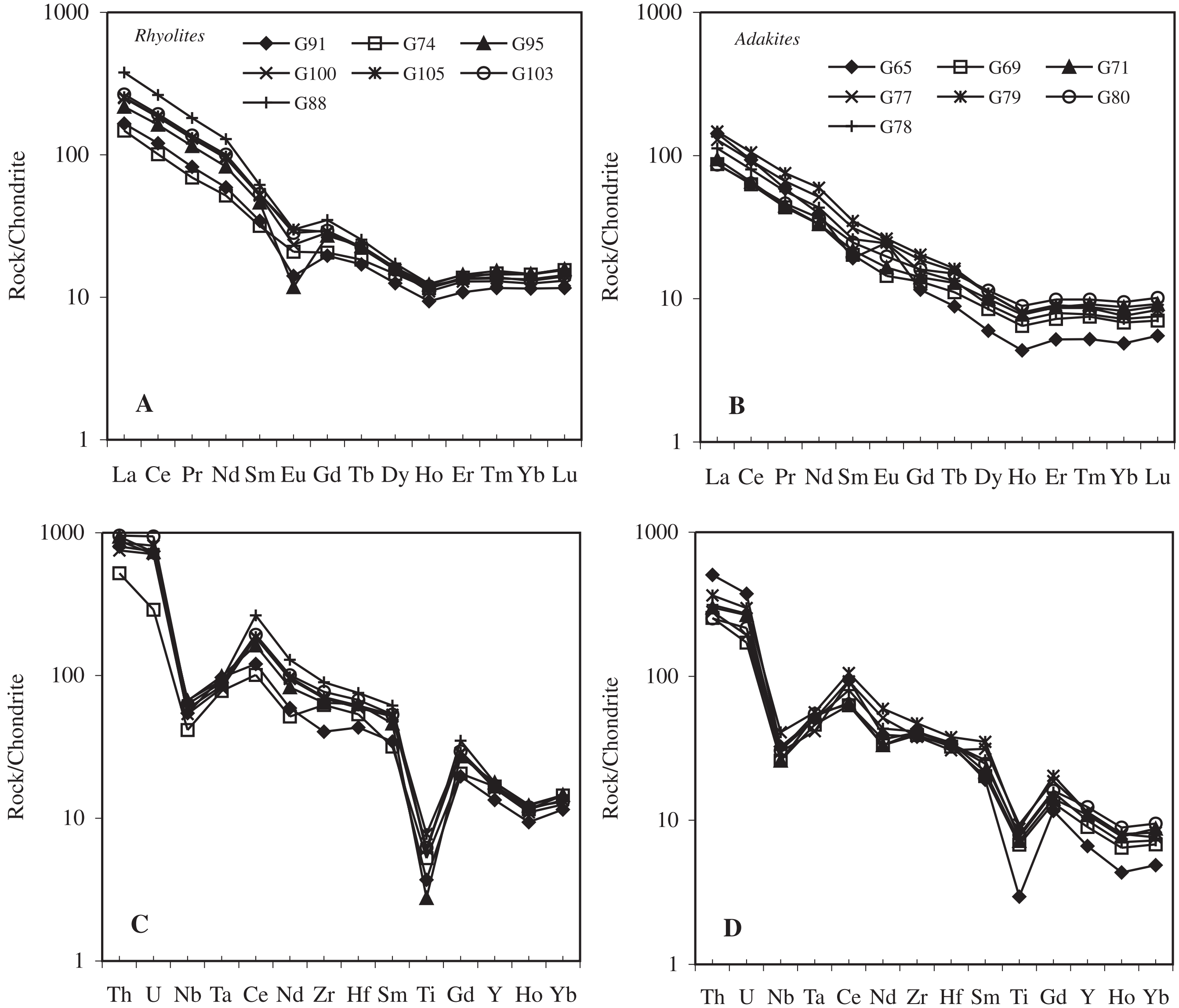

Specifically, rhyolites of similar composition have been documented in the Birch–Uchi greenstone belt, Superior Province, where they occur with an arc basalt–NEB–adakite association (Hollings and Kerrich 2000).

Geodynamic context of adakites

Cenozoic adakites are restricted to oceanic arcs; however, as slab melts rather than slab dehydration-wedge melts, they require special conditions for their petrogenesis. Geodynamic processes proposed to explain the petrogenesis of adakites include (*i*) melting of subducted slab in the upper mantle (adakites of Gulf of California), (*ii*) melting of subducted slab owing to oblique convergence (western Aleutians), (*iii*) melting of oceanic crust during arc–arc collision (Papua New Guinea), (*iv*) melting of oceanic crust during the initiation of a new subduction zone (southern Mindanao and the Philippines), (*v*) melting of oceanic crust owing to slab tearing (Kamchatka), and (*vi*) melting of oceanic crust during flat subduction (Southern Volcanic Zone, Chile) (Defant and Kepezhinskas 2001; Polat and Munker 2004). More recently, Thorkelson and Breitsprecher (2005) proposed slab windows as a site for generation of adakite magmas.

According to Defant and Drummond (1990), Cenozoic adakites are related to the shallow (sometimes oblique) subduction of younger and hotter oceanic crust (<25 Ma old). Under these conditions, basaltic crust melts at 22–26 kbars (1 kbar = 100 MPa), at shallower depth (75–85 km), and at 750–800 °C to generate slab melts of adakitic composition. Geochemical studies carried out on Phanerozoic NEB, andesites, dacites, and adakites from Zamboauga Peninsula of Philippines (Sajona et al. 1993, 1996), southern Andes (Stern and Kilian 1996), Central America (Defant et al. 1992), and western Aleutian Islands (Yogodzinski et al. 1994, 1995) have shown that these rock suites are associated with subduction of young and hot oceanic lithosphere (Table 4).

Table 3. Average compositions of adakites and rhyolites from the Gadwal terrane, and selected averages of other adakites, rhyolites and tonalite–trondhjemite–granodiorite from the literature.

	Dharwar Craton				Superior Province				Global averages		
	Adakite[a]	Rhyolite[a]	Sandur[b]	Kushtagi[c]	Birch-Uchi[d]	Wawa[e]	Lumby Lake[f]	Krist[g]	Adakite[h]	HSA	TTG < 3.0 Ga[i]
SiO_2	66.30	71.71	76.13	69.42	72.35	67.05	74.57	65.48	62.43	64.8	68.36
TiO_2	0.50	0.38	0.26	0.24	0.32	0.46	0.21	0.45	0.67	0.56	0.38
Al_2O_3	15.36	14.39	13.19	17.23	14.01	17.16	13.89	17.89	17.05	16.64	15.52
$Fe_2O_3^{(T)}$	5.40	2.93	0.13	2.07	2.64	3.76	2.24	3.30	3.99	4.75	3.27
MnO	0.07	0.06	0.02	0.03	0.04	0.03	0.03	0.05	0.08	0.08	0.05
MgO	2.22	0.77	0.20	0.72	1.10	1.61	1.34	1.29	3.31	2.18	1.36
CaO	4.90	1.86	1.73	2.16	2.94	3.06	2.3	4.93	6.53	4.63	3.23
K_2O	0.98	4.59	1.54	1.12	2.05	1.75	0.77	4.78	1.42	1.97	2
Na_2O	3.91	3.23	5.60	5.08	4.49	4.98	4.62	1.69	4.25	4.19	4.7
P_2O_5	0.15	0.09	0.08	0.07	0.09	0.15	0.05	0.15	0.26	0.2	0.15
Mg#	0.43	0.33	0.76	0.45	0.44	0.50	0.58	0.46	0.60	0.48	0.45
Cr	15	5.32	99	9	42	68	31	13	82	41	50
Co	13	4	6	47	10	15	4	6	—	—	—
Ni	5.7	1.86	13.6	1.9	25	28	14	14	64	20	21
Rb	54	159	49	29	65	50	—	43	15	52	67
Sr	251	149	205	238	211	640	—	634	1550	565	541
Cs	9.8	4.0	0.92	—	2.5	4.48	—	1.0	—	—	—
Ba	262	535	283	286	511	695	—	430	309	721	847
Sc	8.7	5.9	4.0	2.40	5.5	8.82	8	15	—	—	—
V	129	42	2.1	2.56	41	74	15	63	—	95	52
Ta	0.68	1.25	0.41	0.56	0.4	0.29	0.32	0.28	0.60	—	—
Nb	7.3	14.4	5.4	2.0	4.2	4.92	3.42	4.30	9.70	6	7
Zr	159	269	117	69	103	131	139	116	117	108	154
Hf	3.5	6.3	3.01	1.84	2.79	3.38	3.49	3.5	3.3	—	—
Th	9.1	23	10.1	3.7	5.3	5.0	4.5	2.8	3.9	—	—
U	2.0	5.2	2.5	1.3	1.2	1.15	0.79	0.7	1.2	—	—
Y	15.4	28.5	5.6	5.5	6.0	9.4	4.0	7.6	9.7	10	11
La	25.69	52.46	30.10	13.96	15.61	29.7	11.83	16.70	24.00	19.2	30.8
Ce	46.35	98.72	53.18	25.06	29.72	63.1	22.68	35.58	65.00	37.7	58.5
Pr	4.72	10.27	5.12	2.68	3.06	7.44	2.09	4.15	—	—	—
Nd	18.09	38.41	18.33	10.62	11.14	28	7.50	17	26.00	18.20	23.2
Sm	3.53	7.05	3.03	1.75	1.89	4.78	1.26	3.10	4.70	3.40	3.5
Eu	1.12	1.32	0.82	0.60	0.54	1.22	0.35	1.03	1.37	0.9	0.9
Gd	2.92	5.46	2.14	1.67	1.48	3.34	0.97	2.39	2.30	2.8	2.3
Tb	0.46	0.83	0.26	—	0.20	0.35	0.14	0.23	0.40	—	—
Dy	2.21	4.07	1.02	1.03	1.03	1.83	0.82	1.27	—	1.9	1.6
Ho	0.39	0.72	0.15	—	0.2	0.33	0.13	0.23	—	—	—
Er	1.24	2.34	0.48	0.43	0.53	0.84	0.43	0.72	—	0.96	0.75
Tm	0.19	0.37	0.06	—	0.07	0.12	0.06	0.10	—	—	—
Yb	1.20	2.41	0.39	0.46	0.47	0.73	0.4	0.70	0.81	0.88	0.63
Lu	0.19	0.37	0.06	0.06	0.06	0.11	0.06	0.12	0.09	0.17	0.12
Cu	6.2	3.75	4.0	16.2	—	—	—	23	—	—	—
Zn	54	48	43	37	—	—	—	46	—	—	—
Pb	21	27	51	—	—	—	—	4	—	—	—

Note: HSA, high-silica adakites; TTG, tonalite–trondhjemite–granodiorite.
[a]Present study.
[b]Manikyamba and Khanna (2005).
[c]Naqvi et al. (2006).
[d]Hollings and Kerrich (2000).
[e]Polat and Kerrich (2001).
[f]Type I felsic extrusive from Hollings and Wyman (1999).
[g]Hollings et al. (1999).
[h]Condie (2005).
[i]TTG < 3 Ga from Martin et al. (2005).

Fig. 6. Plots of (A) $(La/Yb)_n$ versus $(Yb)_n$ and (B) Nb/Ta versus Zr/Sm for Gadwal rhyolites and adakites. In (A), averages are from the literature, compiled in Table 4. In (B), fields for island-arc basalts (IAB), adakites, and tonalite–trondhjemite–granodiorite (TTG) are from Foley et al. (2002). Adk., Adakite; HSA, high-silica adakites; avg., average.

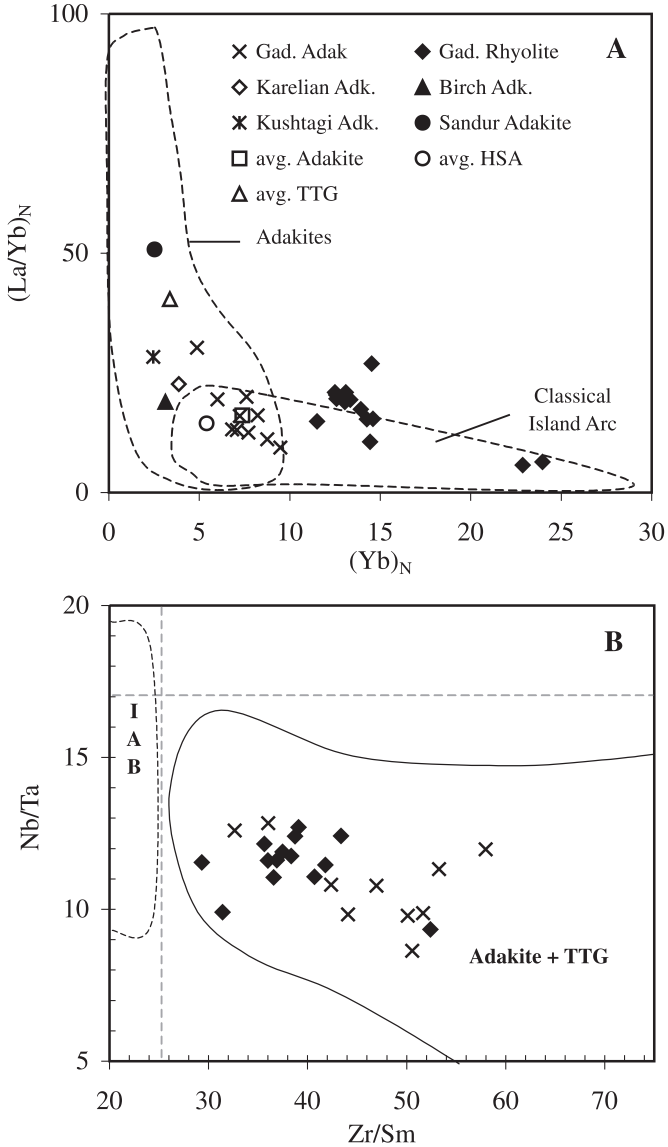

Archean adakites and associated magmas

Adakites are relatively rare and volumetrically minor in Cenozoic arcs (Defant et al. 1992; Drummond et al. 1996; Sajona et al. 1996). Recently, adakites have been documented from a number of Neoarchean terranes, where they are associated with "normal" tholeiitic to calc-alkaline oceanic-arc basalts, and with HMA and (or) NEB. Included are adakites from greenstone belts of the Uchi (Hollings et al. 1999; Hollings and Kerrich 2000) and Wawa (Polat and Kerrich 2002) subprovinces and Ashuanipi complex (Percival et al. 2003), Superior Province, and from the Sandur and Kushtagi greenstone belts, Dharwar craton (Fig. 6A; Table 4; Manikyamba and Khanna 2005; Naqvi et al. 2006). A MORB-arc, back-arc, and basalt–adakite association has been reported from the 2.5 Ga old Wutai greenstone belt, north China (Wang et al. 2004), and adakites are present in the Neoarchaean Karelian greenstone belt, Baltic shield (Samsonov et al. 2005; Table 4).

Boninites, along with NEB and adakites from the Gadwal terrane, extend the number of occurrences of complex volcanic rock suites from the Superior, Baltic, and China cratons to include the Dharwar craton. Consequently, Neoarchaean greenstone terranes could reflect a transition period for the creation of more complex subduction zone processes, involving the interplay of mantle-wedge and slab-derived fluids and melting of wedge and slab (Table 4).

Conclusions

(1) The Gadwal greenstone terrane is dominated by a bimodal association of arc basalts and dacites. New examples of adakites and rhyolites have been documented in the felsic end member.

(2) Gadwal adakites possess the $MgO–SiO_2$ relationships of Cenozoic and other Archean adakites, distinct from sometimes associated high magnesian andesites. They are also characterized by low Y and Yb contents, fractionated REE, and distinctive Cr/Ni, Nb/Ta, and Zr/Sm systematics of Cenozoic adakites.

(3) Positive Eu anomalies rules out contamination by older cratonic crust, endorsing an intraoceanic arc setting as recorded in associated arc basalts.

(4) Cenozoic adakites are generally believed to be slab melts hybridized with peridotitic sub-arc mantle wedge. If this applies to the examples at Gadwal, there was a transition in the convergent margin from slab dehydration-wedge melting for the arc basalts and boninites to slab melting for adakites and Nb-enriched basalts, possibly driven by flattening of the slab or ridge subduction. Gadwal adakites occur with arc basalts and NEB, an association present in other Archean and some Cenozoic arcs.

(5) Rhyolites are the FI type of Lesher et al. (1986), characterized by fractionated REE and pronounced negative Eu anomalies. They represent a distinct magma series from basalts or adakites, and are likely generated as melts of thickened mafic crust at ~40 km under extension.

Table 4. Archaean hot subduction volcanic rocks and their Phanerozoic analogues, expanded from Polat and Kerrich (2006).

	Archaean examples			Phanerozoic examples	
Rock type	Craton	Terrane	Source	Occurrence	Source
Adakite	Dharwar				
		Gadwal	This study	Central America	Defant et al. 1992
		Sandur	Manikyamba and Khanna 2005	Philippines	Sajona et al. 1996
		Kushtagi	Naqvi et al. 2006	Japan	Morris 1995
		Shimoga	Naqvi and Rana Prathap 2007	—	—
	Superior	—	—	Southern Volcanic Zone Andes	Stern and Kilian 1996
		Wabigoon	Tomlinson et al. 1999	Northern Volcanic Zone Andes	Bourdon et al. 2002
		Wabigoon	Ujike and Goodwin 2003	Baja California	Benoit et al. 2002
		Birch–Uchi	Hollings and Kerrich 2000	—	—
		Wawa	Polat and Kerrich 2001	—	—
		Abitibi	Wyman et al. 2002	—	—
		Frotet–Evans	Boily and Dion 2002	—	—
		Ashuanipi	Percival et al. 2003	—	—
	Slave				
		Yellowknife	Cousens et al. 2002	—	—
	Baltic				
		Sumozero–Kenozero	Puchtel et al. 1998	—	—
		Vedlozero–Segozero	Svetov et al. 2004	—	—
	China	Wutaishan	Wang et al. 2004	—	—
High-Mg andesite (HMA)	Dharwar	—	—	Chile	Rogers and Saunders 1989
		Gadwal	Khanna 2006	Philippines	Sajona et al. 1996
	Superior	—	—	Japan	Tatsumi and Maruyama 1989
		Abitibi	Wyman et al. 2002	Antarctic Peninsula	McCarron and Smellie 1998
		Birch–Uchi	Hollings and Kerrich 2000	Baja California	Benoit et al. 2002
		Wawa	Polat and Kerrich 2001	—	—
Nb-enriched basalt (NEB)		—	—	Central America	Defant et al. 1992
	Dharwar	—	—	Northern Kamchatka	Kepezhinskas et al. 1996
		Gadwal	Manikyamba and Khanna 2007	Philippines	Sajona et al. 1996
	Superior	—	—	Baja California	Benoit et al. 2002
		Wabigoon	Wyman et al. 2000	—	—
		Wabigoon	Ujike and Goodwin 2003	—	—
		Birch–Uchi	Hollings and Kerrich 2000	—	—
		Wawa	Polat and Kerrich 2001	—	—
	Baltic				
		Karelian	Shchipansky et al. 2004	—	—
Boninite	Dharwar	—	—	Troodos ophiolite	Beccaluva and Serri 1988
		Gadwal	Manikyamba et al. 2005	Papua NewGuinea ophiolite	Crawford 1989
		Kushtagi	Naqvi et al. 2006	Izu–Bonin–Mariana forearc	Pearce et al. 1992
	Singhbhum	—	—	Betts Cove ophiolite	Bedard 1999
		Bastar	Srivastava et al. 2004	Oman ophiolite	Ishikawa et al. 2002
	Superior	—	—	Ural ophiolites	Spadea and Scarrow 2000
		Abitibi	Kerrich et al. 1998	—	—
		Frotet–Evans	Boily and Dion 2002	—	—
	Pilbara				—

Table 4 (*concluded*).

Rock type	Archaean examples: Craton	Terrane	Source	Phanerozoic examples: Occurrence	Source
		Whundo	Smithies et al. 2005	—	—
	Greenland	Isua	Polat et al. 2002	—	—
	Baltic	Karelian	Shchipansky et al. 2004	—	—
Low-Ti tholeiite (LOTI)	Superior	—	—	Mariana trench, Lau Basin, New Guinea	Beccaluva and Serri 1988
		Abitibi	Kerrich et al. 1998; Wyman 1999	Tasmania	Brown and Jenner 1989
	Baltic	Karelian	Shchipansky et al. 2004	—	—
Picrite	Superior	—	—	Solomon Islands	Ramsay et al. 1984; Shuth et al. 2004
		Wawa	Polat and Kerrich 1999	Central Aleutians	Nye and Reid 1986
	Greenland	—	—	Japan	Yamamoto 1988
		Isua	Polat and Hofmann 2003	Vanuatu arc	Eggins 1993
		Ivisaartoq	Polat et al. 2007	Eastern Kamchatka	Kamenetsky et al. 1995
	China	—	—	Lesser Antilles	Thirlwall et al. 1996
		Zunhua	Polat et al. 2006	—	—

Note: The Phanerozoic examples are grouped by geographic areas not by craton, as for the Archaean examples.

Acknowledgements

The authors are grateful to Dr. V.P. Dimri, Director, National Geophysical Research Institute for permission to publish this paper. Dr. S.M. Naqvi conferred constructive discussions on the petrological and tectonic models. The Department of Science and Technology is acknowledged for providing the research grant to carry out the present work under Deep Continental Studies Programme (ESS/16/143/2001). Drs. V. Balaram and N.N. Murthy are thanked for providing the analytical facilities, and Dr. T.G. Rao and Mr. Kesava Krishna for analyses of these rocks. We are grateful to the Editor and Associate Editor, Drs. B. Jones and J. Greenough, for insights and handling this manuscript. Journal reviewers J-F Moyen, A. Polat, and D. Thorkelson provided incisive critiques that greatly improved this paper. R.K. acknowledges a Natural Sciences and Engineering Research Council of Canada (NSERC) Discovery Grant (7-70835).

References

Abbott, D.H. 1996. Plumes and hotspots as sources of greenstone belts. Lithos, **37**: 13–127.

Anand, M., Gibson, S.A., Subba Rao, K.V., Kelley, S.P., and Dickin, A.P. 2003. Early Proterozoic Melt Generation Processes beneath the Intra-cratonic Cuddapah Basin, Southern India. Journal of Petrology, **44**: 2139–2171.

Arndt, N.T. 1994. Archaean komatiites. *In* Archaean crustal evolution. *Edited by* K.C. Condie. Elsevier, Amsterdam, The Netherlands, pp. 11–44.

Balakrishnan, S., Hanson, G.N., and Rajamani, V. 1990. Pb and Nd isotope constraints on the origin of high Mg and tholeiite amphibolites, Kolar schist belt, southern India. Contributions to Mineralogy Petrology, **107**: 272–292.

Balaram, V., and Gnaneswar Rao, T. 2003. Rapid determination of REEs and other trace elements in geological samples by microwave acid digestion and ICP–MS. Atomic Spectroscopy, **24**: 206–212.

Beccaluva, L., and Serri, G. 1988. Boninitic and low Ti subduction related lavas from intraoceanic arc-back arc systems and low-Ti ophiolites: a reappraisal of their petrogenesis and original tectonic setting. Tectonophysics, **146**: 291–315.

Bedard, J.H. 1999. Petrogenesis of boninites from the Betts Cove ophiolite, Newfoundland, Canada: identification of subducted source components. Journal of Petrology, **40**: 1853–1889.

Bedard, J.H. 2006. Trace element partitioning in plagioclage feldspar. Geochimica et Cosmochimica Acta, **70**: 3717–3742.

Benoit, M., Aguillon-Roblas, A., Calmus, T., Maury, R.C., Bellon, H., Cotton, J., Bourgois, J., and Michaud, F. 2002. Geochemical diversity of late Miocene volcanism in southern Baja California, Mexico: implication of mantle and crustal sources during the opening of an asthenospheric window. Journal of Geology, **110**: 627–648.

Boily, M., and Dion, C. 2002. Geochemistry of boninite-type volcanic rocks in the Frotet–Evans greenstone belt, Opatica subprovince, Quebec: implications for the evolution of Archaean greenstone belt. Precambrian Research, **115**: 349–371.

Bourdon, E., Eissen, J.P., Monzier, M., Robin, C., Martin, H., Cotton, J., and Hall, M.L. 2002. Adakite like lavas from Antisana volcano (Ecuador): evidence for slab melt metasomatism beneath the Andean Northern volcanic zone. Journal of Petrology, **43**: 199–217.

Brown, A.V., and Jenner, G.A. 1989. Geological setting, petrology and chemistry of Cambrian boninite and low-Ti tholeiitic lavas in western Tasmania. *In* Boninites and related rocks. *Edited by* A.J. Crawford. Unwin Hyman, London, UK., pp. 233–263.

Chalapathi Rao, N.V., Miller, J.A., Gibson, S.A., Pyle, D.M., and Madhavan, V. 1999. Precise $^{40}Ar/^{39}Ar$ age determinations of the Kotakonda kimberlites and Chelima lamproite, India: implication to the timing of mafic dyke swam emplacement in the eastern Dharwar craton. Journal of the Geological Society of India, **53**: 425–432.

Condie, K.C. 2005. TTGs and adakites: are they both slab melts? Lithos, **80**: 33–44.

Cousens, B., Facey, K., and Falck, H. 2002. Geochemistry of the late Archean Banting Group, Yellowknife greenstone belt, Slave Province, Canada: simultaneous melting of the upper mantle and juvenile mafic crust. Canadian Journal of Earth Sciences, **39**: 1635–1656.

Crawford, A.J., Fallon, T.J., and Green, D.H. 1989. Classification, petrogenesis and tectonic setting of boninites. *In* Boninites and related rocks. *Edited by* A.J. Crawford. Unwin Hyman, London, UK., pp. 1–49.

Defant, M.J., and Drummond, M.S. 1990. Derivation of some modern arc magmas by melting of young subducted lithosphere. Nature (London), **347**: 662–665.

Defant, M.J., and Kepezhinskas, P. 2001. Evidence suggests slab melting in arc magmas. EOS, **82**: 65–69.

Defant, M.J., Jackson, T.E., Drummond, M.S., De Boer, J.Z., Bellon, H., Feigemson, M.D., Maury, R.C., and Stewart, R.H. 1992. The geochemistry of young volcanism throughout west Panama and southeastern Costa Rica: an overview. Journal of the Geological Society (of London), **149**: 569–579.

DePaolo, D.J. 1980. Crustal growth and mantle evolution; inferences from models of element transport and Nd and Sr isotopes. Geochimica et Cosmochimica Acta, **44**: 1185–1196.

Dostal, J., Strong, D.F., and Jamieson, R.A. 1980. Trace element mobility in the mylonite zone within the ophiolite aureole, St. Anthony Complex, Newfoundland. Earth and Planetary Science Letters, **49**: 188–192.

Drummond, M.S., and Defant, M.J. 1990. A model for trondhjemite-tonalite-dacite genesis and crustal growth via slab melting: Archaean to modern comparisons. Journal of Geophysical Research, **95**: 21503–21521.

Drummond, M.S., Defant, M.J., and Kepezhinskas, P.K. 1996. Petrogenesis of slab derived-tonalite-dacite-adakite magmas. Transactions of the Royal Society of Edingburgh, Earth Sciences, **87**: 205–215.

Eggins, S.M. 1993. Origin and differentiation of Picritic arc magmas, Ambae (Aoba), Vanuatu. Contributions to Mineralogy and Petrology, **114**: 79–100.

Foley, S., Barth, M.G., and Jenner, G.A. 2000. Rutile/melt partition coefficient for trace elements and an assessment of the influence of rutile on the trace element characteristics of subduction zone magmas. Geochimica et Cosmochimica Acta, **64**: 933–938.

Foley, S., Tiepolo, M., and Vannucci, R. 2002. Growth and early continental crust controlled by melting of amphibolite in subduction zones. Nature (London), **417**: 837–840.

Gao, S., and Wedepohl, K.H. 1995. The negative Eu anomaly in Archaean sedimentary rocks: implications fro decomposition, age and importance of their granitic sources. Earth and Planetary Science Letters, **133**: 81–94.

Gutscher M-A., Maury, R., Eissen, J-P., and Bourdon, E. 2000. Can slab melting be caused by flat subduction? Geology, **28**: 535–538.

Hart, T.R., Gibson, H.L., and Lesher, C.M. 2004. Trace element geochemistry and petrogenesis of felsic volcanic rocks associated with volcanogenic massive Cu–Zn–Pb sulfide deposits. Economic Geology, **99**: 1003–1013.

Haschke, M., Siebel, W., Gunther, A., and Scheuber, E. 2002. Repeated crustal thickening and recycling during the Andean orogeny in north Chile (21°–26°). Journal of Geophysical Research, **107**; B1, p. ECV 6-1-18, doi 10.1029/2001JB000328.

Hawkesworth, C.J., Gallagher, K., Hergt, J.M., and McDermott, F. 1993. Mantle and slab contributions in arc magmas. Annual Review of Earth Planetary Sciences, **21**: 175–204.

Hollings, P., and Wyman, D. 1999. Trace element and Sm–Nd systematics of volcanic and intrusive rocks from the 3 Ga Lumby Lake greenstone belt, Superior Province: evidence for Archaean plume-arc interaction. Lithos, **46**: 189–213.

Hollings, P., and Kerrich, R. 2000. An Archaean arc basalt – Nb enriched basalt – adakite association: the 2.7 Ga Confederation assemblage of the Birch–Uchi greenstone belt, Superior Province. Contributions to Mineralogy and Petrology, **139**: 208–226.

Hollings, P., Wyman, D., and Kerrich, R. 1999. Komatiite–basalt–rhyolite volcanic associations in northern Superior Province greenstone belts: significance of plume–arc interaction in the generation of the proto continental Superior Province. Lithos, **46**: 137–161.

Humphris, S. E., and Thompson, G. 1978. Trace element mobility during hydrothermal alteration of oceanic basalts. Geochimica et Cosmochimica Acta, **42**: 127–136.

Ishikawa, T., Nagaishi, K., and Umino, S. 2002. Boninitic volcanism in the Oman ophiolite: implications for thermal conditions during transition from spreading ridge to arc. Geology, **30**: 899–902.

Jayananda, M., Moyen, J.-F., Martin, H., Peucat, J.-J., Auvray, B., and Mahabaleswar, B. 2000. Late Archaean (2550–2520 Ma) juvenile magmatism in the eastern Dharwar Craton, Southern India: constraints from geochronology, Nd–Sr isotopes and whole rock geochemistry. Precambrian Research, **99**: 225–254.

Jenner, G.A., Longerich, H.P., Jackson, S.E., and Fryer, B.J. 1990. ICP–MS—a powerful tool for high precision trace element analysis in Earth Sciences: evidence from analysis of selected USGS reference samples. Chemical Geology, **83**: 133–148.

Jochum, K.P., Arndt, N.T., and Hofman, A.W. 1991. Nb–Th–La in komatiites and basalts: constraints on komatiite petrogenesis and mantle evolution. Earth and Planetary Science Letters, **107**: 272–289.

Kay, S.M., Mpodois, C., Ramos, V.A., and Munizaga, F. 1991. Magma source variations for mid-late Teriay magmatic rocks associated with a shallowing subduction zone and a thickening crust in the central Andes (28° to 33°). *In* Andean magmatism and its tectonic setting. *Edited by* R.S. Harmon and C.W. Rapela. Geological Society of America, Boulder, Colo. Special Paper 265, pp. 113–137.

Kamenetsky, V.S., Sobolev, A.V., Joron, J.-L., and Semet, M.P. 1995. Petrology and geochemistry of Cretaceous ultramafic volcanic rocks from eastern Kamchatka. Journal of Petrology, **36**: 637–662.

Kepezhinskas, P., Defant, M.J., and Drummond, M.S. 1996. Progressive enrichment of island arc mantle by melt-peridotite interaction inferred from Kamchatka xenoliths. Geochimica et Cosmochimica Acta, **60**: 1217–1229.

Kerrich, R., and Fryer, B.J. 1979. Archaean precious metal hydrothermal systems Dome Mine Abitibi greenstone belt: II REE and oxygen isotope relations. Canadian Journal of Earth Sciences, **16**: 440–458.

Kerrich, R., Wyman, D., Fan, J., and Bleeker, W. 1998. Boninite series: low Ti-tholeiite association from the 2.7 Ga Abitibi greenstone belt. Earth and Planetary Science Letters, **164**: 303–316.

Khanna, T.C. 2006. Geochemistry and tectonic setting of the metavolcanic rocks of Gadwal greenstone belt. Unpublished Ph.D. thesis, Osmania University, Hyderabad, India.

Klepeis, K.A., Clarke, G.L., and Rushmer, T. 2003. Magma transport and coupling between deformation and magmatism in the continental lithosphere. GSA Today, **13**, 4–11.

Knowles, J. 1995. Fusion partielle de la croute oceanique dans une zone de subduction: approche par les desequillibres U–Th. Unpublished memoir, University of Clermont-Ferrand, France.

Lafleche, M. R., Dupuy, C., and Dostal, J. 1992. Tholeiitic volcanic rocks of the late Archaean Blake River group, southern Abitibi greenstone belt: origin and geodynamic implications. Canadian Journal of Earth Sciences, **29**: 1448–1458.

Lesher, C.M., Goodwin, A.M., Campbell, I.H., and Gorton, M.P. 1986. Trace element geochemistry of ore associated and barren, felsic metavolcanic rocks in the Superior Province, Canada. Canadian Journal of Earth Sciences, **23**: 222–237.

Longerich, H. P., Jenner, G. A., Fryer, B. J., and Jackson, S. E. 1990. Inductively Coupled Plasma-Mass Spectrometric Analysis of geological samples: a critical evaluation based on case studies. Chemical Geology, **83**: 105–118.

Ludden, J., Gelienas, L., and Trudel, P. 1982. Archaean metavolcanics from the Rouyn-Noranda District, Abitibi greenstone belt, Quebec: 2 mobility of trace elements and petrogenetic constraints. Canadian Journal of Earth Sciences, **19**: 2276–2287.

Macpherson, C.G., Dreher, S.T., and Thirlwall, M.F. 2006. Adakites without slab melting: high pressure differentiation of island arc magmas, Mindanao, the Philippines. Earth and Planetary Science Letters, **243**: 581–593.

Manikyamba, C., and Khanna, T.C. 2005. Geochemical Characteristics of Adakites from Sandur schist belt (SSB)—implications on their tectonic setting. *In* Proceedings of the National Seminar on Geology and Energy Resources of NE India: Progress and Perspectives, Kohima, Nagaland, India. pp. 99–100.

Manikyamba, C., and Khanna, T. C. 2007. Crustal Growth Processes as illustrated by the Neoarchaean intraoceanic magmatism from Gadwal greenstone belt, Eastern Dharwar Craton, India. Gondwana Research, **11**: 476–491.

Manikyamba, C., Kerrich, R., Naqvi, S.M., and Ram Mohan, M. 2004. Geochemical systematics tholeiitic basalts from the 2.7 Ga Ramagiri–Hungund composite greenstone belt, Dharwar craton. Precambrian Research, **134**: 21–39.

Manikyamba, C., Naqvi, S.M., Subba Rao, V., Ram Mohan, M., Tarun C Khanna, Rao, T.G., and Reddy, G.L.N. 2005. Neoarchaean boninites—Implications for Archaean subduction processes. Earth and Planetary Science Letters, **230**: 65–83.

Martin, H. 1986. Effect of steeper Archaean geothermal gradient on geochemistry of subduction-zone magmas. Geology, **14**: 753–756.

Martin, H. 1999. Adakitic magmas: modern analogues of Archaean granitoids. Lithos, **46**: 411–429.

Martin, H., Smithies, R.H., Rapp, R., Moyen, J.-F., and Champion, D. 2005. An overview of adakites, tonalite–trondhjemite–granodiorite (TTG) and sanikoid:relationships and some implications for crustal evolution. Lithos, **79**: 1–24.

Matin, A. 2001. Structure of the Gadwal schist belt, Eastern Dharwar craton, Mahbubnagar and Kurnool District, Andhra Pradesh. Indian Journal of Geology, **73**: 199–205.

Maury, R.C., Sajona, F.G., Pubellier, M., Bellon, H., and Defant, M.J. 1996. Fusion de la croute dans les zones de subduction/collision recentes: 1'example de Mindanao (Philippines). Geological Society of France Bulletin, **167** (5): 579–595.

McCarron, J.J., and Smellie, J.L. 1998. Tectonic implications of fore-arc magmatism and generation of high-Magnesian andesites: Alexander Island, Antarctica. Journal of Geological Society (of London), **155**: 269–280.

Melcher, F., and Meisel, T. 2004. A metamorphosed early Cambrian crust-mantle transition in the Eastern Alps, Austria. Journal of Petrology, **45**: 1689–1723.

Morris, P.A. 1995. Slab melting as an explanation of Quartenary volcansim and aseismicity in Southwestern Japan. Geology**, 23**: 395–398.

Moyen, J-F., and Stevens, G. 2006. Experimental constraints on TTG petrogenesis: Implications for Archean geodynamics. *In* Archean geodynamics and environments. *Edited by* K. Benn, J-C Maraschal, and K.C. Condie. American Geophysical Monograph 164, pp. 149–175.

Murphy, J.B., and Hynes, A.J. 1986. Constrasting secondaray mobility of Ti, P, Zr, Nb and Y in two metabasaltic suites in the Appalachians. Canadian Journal of Earth Sciences, **23**: 1138–1144.

Naqvi, S.M. 2005. Geology and evolution of Indian Plate: Hadean to Holocene- 4 Ga to 4 Ka. Capital Publishing Company, Delhi, India.

Naqvi, S.M., and Rana Pratap, J.G. 2007. The geochemistry of adakites from Neoarchean active continental margin of Shimoga schist belt, western Dharwar caton, India: implications for the genesis of TTG. Precambrian Research, **156**: 32–54.

Naqvi, S.M., and Rogers, J.J.W. 1987. Precambrian geology of India. Oxford Monographs on Geology and Geophysics, Oxford University Press, Oxford, UK.

Naqvi, S.M., Manikyamba, C., Gnaneshwar Rao, T., Subba Rao, D.V., Ram Mohan, M., and Srinivasa Sarma, D. 2002. Geochemical and isotopic constraints of Neoarchaean fossil plume for evolution of volcanic rocks of Sandur greenstone belt, India. Journal of the Geological Society of India, **60**: 27–56.

Naqvi, S.M., Khan, R.M.K., Manikyamba, C., Ram Mohan, M., and Khanna, T.C. 2006. Geochemistry of the Neoarchaean high-Mg basalts, boninites and adakites form the Kushtagi–Hungund greenstone belt of the eastern Dhawar craton (EDC); implications for the tectonic setting. Journal of Asian Earth Sciences, **27**: 25–44.

Nye, C.J., and Reid, M.R. 1986. Geochemistry of primary and least fractionated lavas from Okmaok volcano, Central Aleutians: implications for arc magma genesis. Journal of Geophysical Research, **91**: 10 271 – 10 287.

Pearce, J.A., and Peate, D.W. 1995. Tectonic implications of the composition of volcanic arc magmas. Annual Review of Earth and Planetary Sciences, **23**: 251–285.

Pearce, J.A., van der Laan, S., Arculus, R.J., Murton, B.J., Ishii, T., and Peate, D.W. 1992. Boninite and harzburgite from Leg 125 (Bonin–Mariana fore-arc): a case study of magma genesis during the initial stage of subduction. Proceedings of the Ocean Drilling Program Scientific Research, **125**: 623–659.

Percival, J.A., Stern, R.A., and Rayner, N. 2003. Archaean adakites from the Ashuanipi complex, Eastern Superior Province, Canada: geochemistry, geochronology and tectonic significance. Contributions to Mineralogy and Petrolology, **140**: 265–280.

Polat, A., and Hofmann, A.W. 2003. Alteration and geochemical patterns in the 3.7–3.8 Ga Isua greenstone belt, west Greenland. Precambrian Research, **126**: 197–218.

Polat, A., and Kerrich, R. 1999. Formation of an Archaean tectonic mélange in the Schreiber–Hemlo greenstone belt, superior Province, Canada: implications for Archaean subduction–accretion process. Tectonics, **18**: 733–755.

Polat, A., and Kerrich, R. 2001. Magnesian andesites, Nb-enriched basalt – andesites, and adakites from late-Archaean 2.7 Ga Wawa greenstone belts, Superior Province, Canada: implications for late Archaean subduction zone petrogenetic processes. Contributions to Mineralogy and Petrology, **141**: 36–52.

Polat, A., and Kerrich, R. 2002. Nd-isotope systematics of ~2.7 Ga adakites, magnesian andesites, and arc basalts, Superior Province: evidence for shallow crustal recycling at Archean subduction zones. Earth and Planetary Science Letters, **202**: 345–360.

Polat, A., and Kerrich, R. 2006. Reading the geochemical fingerprints of Archean hot subduction volcanic rocks: Evidence for accretion and crustal recycling in a mobile tectonic regime. *In* Archean geodynamics and environments. *Edited by* K. Benn, J-C. Mareschal, and K.C. Condie. American Geophysical Union, Geophysical Monograph 164, pp. 189–213.

Polat, A., and Munker, C. 2004. Hf-Nd isotope evidence for contemporaneous subduction processes in the source of late Archaean arc lavas from the Superior Province, Canada. Chemical Geology, **213**: 403–429.

Polat, A., Hofmann, A.W., and Rosing, M.T. 2002. Boninite-like volcanic rocks in the 3.7–3.8 Ga Isua greenstone belt, West Greenland: geochemical evidence for intra-oceanic subduction zone processes in the early Earth. Chemical Geology, **184**: 231–254.

Polat, A., Herzberg, C., Munker, C., Rodgers, R., Kusky, T., Li, J., Fryer, B., and Delaney, J. 2006. Geochemical and petrological evidence for supra-subduction zone origin of Neoarchean (ca. 2.5 Ga) peridotites, central orogenic belt, North China craton. Geological Society of America Bulletin, **118**: 771–784.

Polat, A., Appel, P.W.U., Frei, R., Pan, Y., Dilek, Y., Ordonez-Caldeeron, J.C., Fryer, B., and Raith, J.G. 2007. Field and geochemical characteristics of the Mesoarchean (~3075 Ma) Ivisaartoq greenstone belt, southern West Greenland: evidence for seafloor hydrothermal alteration in suprasubduction oceanic crust. Gondwana Research, **11**: 69–91.

Puchtel, I.S., Hofmann, A.W., Mezger,K., Jochum, K.P., Shchipansky, A.A., and Samsonov, A.V. 1998. Oceanic plateau model for continental crustal growth in the Archaean: a case study from the Kostomuksha greenstone belt, NW Baltic Shield. Earth and Planetary Science Letters, **155**: 57–74.

Ramakrishnan, M. 2003. Tectonics of Southern Granulite Terrain–Kuppam-Palani Geotransect. Geological Society of India, Memoir 50.

Ramsay, W.R.H., Crawford, A.J., and Foden, J.D. 1984. Field setting, mineralogy, chemistry and genesis of arc picrites, New Georgia, Solomon Islands. Contributions to Mineralogy and Petrology, **88**: 386–402.

Rapp, R.P., Shimzu, N., Norman, M.D., and Applegate, G.S. 1999. Reaction between slab-derived melts and peridotite in the mantle wedge: experimental constraints at 3.8 Gpa. Chemical Geology, **160**: 335–356.

Rapp, R.P., Shimizu, N., and Norman, M.D. 2003. Growth of early continental crust by partial melting of eclogite. Nature, **425**: 605–609.

Richards, J.P., and Kerrich, R. In Press. Adakites: their diverse origin and questionable role in metallogenesis. Economic Geology.

Richards, J.P., Boyce, A.J., and Pringle, M.S. 2001. Geologic evolution of the Escondida area, northern Chile: a model for spatial and temporal localization of porphyry Cu mineralization. Economic Geology, **96**: 271–305.

Rogers, G., and Saunders, A.D. 1989. Magnesian andesites from Mexico, Chile, and the Aleutian Islands: implications for magmatism associated with ridge–trench subduction. *In* Boninites and related rocks. *Edited by* A.J. Crawford. Unwin Hyman, London, UK. pp. 416–445.

Sajona, F.G., Maury, R.C., Bellon, H., Cotton, J., Defant, M.J., and Pubellier, M. 1993. Initiation of subduction and generation of slab-melts in western and eastern Mindanoa, Philippines. Geology, **21**: 1007–1010.

Sajona, F.G., Maury, R.C., Bellon, H., Cotton, J., and Defant, M. 1996. High field strength element enrichment of Pliocene—Pleistocene Island arc basalts, Zamboanga Peninsula, Western Mindanao (Philippines). Journal of Petrology, **37**: 693–726.

Samaniego, P. 1997. Interactions entre les magmas adakitiques et calco-alcalins: geochimie des complexes volcaniques du Cayambe et du Moranda-Fuya (Equateur). Unpublished memoir, University of Clermont-Ferrand, France.

Samsonov, A.V., Bogima, M.M., Bibikova, E.V., Petrova, A.Yu., and Shchipansky, A.A. 2005. The relationship between adakitic, calc-alkaline volcanic rocks and TTGs: implications for the tectonic setting of the Karelian greenstone belt, Baltic Schield. Lithos, **79**: 83–106.

Schuth, S. Rohrbach, A., Munker, C., Ballhaus, C., Garben-Schonberg, D., and Qopoto, C. 2004. Geochemical constraints on the petrogenesis of arc picrites and basalts, New Georgia group, Solomon Islands. Contributions to Mineralogy and Petrology, **148**: 288–304.

Shchipansky, A.A., Samsonov, A.V., Bibikova, E.V., Babarina, I.I., Konilov, A.N., Krylov, K.A., Slabunov, A.I., and Bogina, M.M. 2004. Boninite hosting partial subduction zone ophiolite sequences from the north Karelian greenstone belt, NE Baltic Shield, Russia. *In* Precambrian ophiolites and related rocks. *Edited by* T.M. Kusky. Elsevier, Amsterdam, The Netherlands, pp. 425–486.

Smithies, R.H., Champion, D.C., and Cassidy, K.F. 2003. Formation of Earth's early Archaean continental crust. Precambrian Research, **127**: 89–101.

Smithies, R.H., Champion, D.C., van Kranendonk, N.J., Howard, H.M., and Hickman, A.H. 2005. Modern style subduction processes in the Mesoarchaean: geochemical evidence from the 3.12 Ga Whundo intra-oceanic arc. Earth and Planetary Science Letters, **231**: 221–237.

Spadea, P., and Scarrow, J.H. 2000. Early Devonian boninites from the Magnitogorsk Arc, Southern Urals (Russia): implications for early development of a collisional orogen. *In* Ophiolites and oceanic crust: new insights from field studies and the Ocean Drilling Programme. *Edited by* Y. Dilek, E.M. Moores, D. Elthon and A. Nicolas. Geological Society of America, Boulder, Colo., Special Paper 349, pp. 461–472.

Srinivasan, K.N. 1990. Geology of Veligallu and Gadwal schist belts. Records of the Geological Survey of India, **123**: 5.

Srivastava, R.K., Singh, R.K., and Verma, S.P. 2004. Neoarchaean volcanic rocks from the southern Bastar greenstone belt, central India: petrological and tectonic significance. Precambrian Research, **131**: 305–322.

Stern, C.R., and Kilian, R. 1996. Role of the subducted slab, mantle wedge and continental crust in the generation of adakites from the Austral Volcanic Zone. Contributions to Mineralogy and Petrology, **123**: 263–281.

Stevenson, R., Henry, P., and Gariepy, C. 1999. Assimilation-fractional crystallization origin of Archean Sanukitoid Suites: Western Superior Province Canada. Precambrian Research, **96**: 83–99.

Sun, S.S., and McDonough, W.F. 1989. Chemical and isotopic systematics of oceanic basalts: implications for mantle composition and processes. *In* Magmatism in the ocean basin. *Edited by* A.D. Saunders and M.J. Norry. Geological Society (of London), Special Publication 42, pp. 313–345.

Svetov, S.A., Huhma, H., Svetova, A.I., and Nazarova, T.N. 2004. The oldest adakites of the Fennoscandian Shield. Doklady Earth Sciences, **397A**: 878–882.

Tatsumi, Y., and Maruyama, S. 1989. Boninites and high-Mg andesites: tectonic and petrogenesis. *In* Boninites and related rocks. *Edited by* A.J. Crawford. Unwin Hyman, London, UK., pp. 50–71.

Taylor, S.R., and McLennan, S.M. 1985. The continental crust: its composition and evolution. Blackwell, Oxford, UK.

Thirlwall, M.F., Graham, A.M., Arculus, R.J., Harmon, R.S., and Macpherson, C.G. 1996. Resolution of the effects of the crustal assimilation, sediment subduction and fluid transport in arc magmas: Pb-Sr-Nd-O isotope geochemistry of Grenada, Lesser Antilles. Geochimica et Cosmochimica Acta, **60**: 4785–4810.

Thorkelson, D.J., and Breitsprecher, K. 2005. Partial melting of slab window margins: genesis of adakitic and non-adakitic magmas. Lithos, **79**: 25–41.

Tomlinson, K.Y., Hughes, D.J., Thurston, P.C., and Hall, R.P. 1999. Plume magmatism and crustal growth at 2.9–3.0 Ga in the Steep Rock and Lumby Lake area, western Superior Province. Lithos, **46**: 103–136.

Ujike, O., and Goodwin, A.M. 2003. Origin of Archaean adakites and NEBA from the upper Keewatin assemblage, the Lake of the Woods greenstone belt, western Wabigoon subprovince. Geochimica et Cosmochimica Acta, **67**: A503.

Wang, Z., Wilde, S.A., Wang, K., and Yu, L. 2004. A MORB-arc basalt-adakite association in the 2.5 Ga Wutai greenstone belt: late Archaean magmatism and crustal growth in the North China Craton. Precambrian Research, **131**: 323–343.

Whalen, J.B., Percival, J.A., McNicoll, V.J., and Longstaffe, F.J. 2002. A mainly crustal origin for tonalitic granitoid rocks, Superior Province, Canada: implications for late Archean tectonomagmatic processes. Journal of Petrology, **43**: 1551–1570.

Wyman, D.A. 1999. A 2.7 Ga depleted tholeiite suite: evidence of plume-arc interaction in the Abitibi greenstone belt, Canada. Precambrian Research, **97**: 27–42.

Wyman, D.A., Ayer, J.A., and Devaney, J.R. 2000. Niobium-enriched basalts from the Wabigoon subprovince, Canada: evidence for adikitic metasomatism above an Archaean subduction zone. Earth and Planetary Science Letters, **179**: 21–30.

Wyman, D.A., Kerrich, R., and Polat, A. 2002. Assembly of Archaean cratonic mantle lithosphere and crust: plume-arc interaction in the Abitibi–Wawa subduction–accretion complex. Precambrian Research, **115**: 37–62.

Yamamoto, M. 1988. Picritic primary magma and its source mantle for Oshima–Oshima and back-arc side volcanoes, northwest Japan. Contributions to Mineralogy and Petrology, **99**: 352–359.

Yogodzinski, G.M., Volynets, O.N., Koloskov, A.V., Seliverstov, N.I., and Matvenkov, V.V. 1994. Magnesian andesites and subduction component in a strongly cacl-alkaline series at Piip volcano, far western Aleutians. Journal of Petrology, **35**: 163–204.

Yogodzinski, G.M., Kay, R.W., Volynets, O.N., Kolosov, A.V., and Kay, S.M. 1995. Magnesian andesite in the western Aleutian Komandorsky region: implications for slab melting and processes in the mantle wedge. Geological Society of America Bulletin, **107**: 505–519.

Zachariah, J.K., Hanson, G.N., and Rajamani, V. 1995. Postcrystallization disturbance in the neodymium and lead isotope systems of metabasalts from the Ramagiri schist belt, southern India. Geochimica et Cosmochimica Acta, **59**: 3189–3203.